Meteoritics & Planetary Science 34, 497–525 (1999)

Invited Review

Laboratory simulation of the physical processes occurring on and near the surfaces of comet nuclei

DEREK W. G. SEARS[1]*, HERMANN W. KOCHAN[2] AND WALTER F. HUEBNER[3]

[1]Cosmochemistry Group, Department of Chemistry and Biochemistry, University of Arkansas, Fayetteville, Arkansas 72701, USA
[2]Deustches Zentrum für Luft- und Raumfahrt e. V., Institut for Raumsimulation, D-51147 Köln, Germany
[3]Southwest Research Institute, P.O. Drawer 28510, San Antonio, Texas 78228-0510, USA
*Correspondence author's e-mail address: cosmo@uafsysb.uark.edu

(Received 1998 September 21; accepted in revised form 1999 February 17)

Abstract–Laboratory comet simulation experiments are discussed in the context of theoretical models and recent ground-based and spacecraft observations, especially the *Giotto* observations of P/Halley. The set-up of various comet simulation experiments is reviewed. A number of small-scale experiments have been performed in many laboratories since the early 1960s. However, the largest and most ambitious series of experiments were the comet simulation experiments known as KOSI (German = Kometen Simulation). These experiments were prompted by the appearance of Comet P/Halley in 1986 and in planning for the European Space Agency's *Rossetta* mission that was originally scheduled to return samples. They were performed between 1987 and 1993 using the German Space Agency's (DLR) space hardware testing facilities in Cologne. As with attempts to reproduce any natural phenomenon in the laboratory, there are deficiencies in such experiments while there are major new insights to be gained. Simulation experiments have enabled the development of methods for making comet analogues and for exploring the properties of such materials in detail. These experiments have provided new insights into the morphology and physical behavior of aggregates formed from silicate grains likely to exist in comets. Formation of a dust mantle on the surfaces and a system of ice layers below the mantle caused by chemical differentiation have been identified after the insolation of the artificial comet. The mechanisms for heat transfer between the comet's surface and its interior, the associated gas diffusion from the interior of the surface, and compositional, structural, and isotopic changes that occur near the surface have been described by modeling the experimental results. The mechanisms of the ejection of dust and ice grains from the surface and the importance of gas-drag in propelling grains have also been explored.

Where the telescope ends,
The microscope begins.
Who is to say of the two,
Which has the grander view.
Victor Hugo

CONTENTS

INTRODUCTION

The study of comets has played a crucial role in establishing the nature of the solar system and gravitational theory (Hoskins, 1997). Comets may have played a part in determining the Earth's inventory of volatiles (Prinn and Fegley, 1989) and perhaps even in the origin of life on Earth (Oró, 1961; Ponnamperuma, 1981). Some short-period comets may evolve into asteroids (Degewij and Tedesco, 1979; Weismann *et al.*, 1989; Wetherill, 1991), linking interstellar space to the inner solar system, and thus some may be the parent bodies of meteorites and micrometeorites (Campins and Swindle, 1998).

Three factors have resulted in an enormous growth in our understanding of comets over the last two decades. (1) The armada of spacecraft that encountered Comet P/Halley in 1986, two from Russia (*Vega 1* and *Vega 2*), two from Japan (*Sakigake* and *Suisei*), one from Europe (*Giotto*), and the *International Comet Explorer (ICE)* from the USA. Details of past and planned comet missions appear in Table 1. (2) The European Space Agency's decision to make a comet probe one of its "cornerstone" missions. (3) A spectacular series of comets (Kohoutek, Halley, Hyakutake, Shoemaker-Levy 9, and Hale-Bopp).

These two decades of activity have resulted in numerous books on comet research (Wilkening, 1982; Ponnamperuma, 1981; Newburn *et al.*, 1991; Lagerkvist *et al.*, 1986; Battrick *et al.*, 1986; ESA-SP 249, 1986; Rolfe and Battrick, 1987; Delsemme, 1977; Grewing *et al.*, 1988; Hunt and Guyenne, 1989), much of which was summarized in Huebner (1990). It is almost certain that the upcoming decade will be equally important, with the *Rosetta* (Atzei *et al.*, 1992), *Stardust*, *Deep Space 1*, *Champollion/Deep Space 4*, and *Contour* spacecraft missions, *Stardust* involving sample return. Stöffler (1991) has discussed the requirements and operation of a curatorial facility for returned comet samples. *Rosetta* was originally planned as a sample return mission but will now conduct *in situ* experiments from a lander on the surface of the nucleus and extended observations from orbit.

The last two decades of comet research have also been characterized by an increasingly important role for ground-based studies; theoretical modeling, thermodynamic and structural studies of ices, and studies of comet analogue materials under conditions approximating those of the comets. Of course, these three areas are closely related, the last two especially. Theoretical modeling has been reviewed many times (Keller, 1990; Donn, 1991; Colangeli *et al.*, 1992a; Rickman, 1991) and two books have been dedicated to the properties of ices of relevance to comets and planetary science (Klinger *et al.*, 1985; Schmitt *et al.*, 1998). In this paper, we review laboratory comet simulation experiments. These experiments have been extremely successful, notwithstanding several limitations, and are of particular interest to the community that will eventually examine samples *in situ* or returned to Earth. We will review the procedures and the results, try to place some of the results in the context of astronomical observations of comets, and discuss the role and limitations of simulation experiments. We will also identify possibilities for future work. But first we very briefly review some current thinking on the formation and evolution of comets.

TABLE 1. Spacecraft missions to comets and some details.

Spacecraft	Launch date	Encounter date	Comet	Reference
Past				
ICE	Aug 78	Sep 85	G-Z	Brandt *et al.* (1988)
ICE	Aug 78	Mar 86	Halley	Brandt *et al.* (1988)
Giotto	Jul 85	Mar 86	Halley	Reinhard (1988)
Giotto	Jul 85	Jul 92	G-S	
Sakigake	Jan 85	Mar 86	Halley	Hirao and Itoh (1986)
Suisei	Aug 85	Mar 86	Halley	Hirao and Itoh (1986)
Vega 1	Dec 84	Mar 86	Halley	Sagdeev (1988)
Vega 2	Dec 84	Mar 86	Halley	Sagdeev (1988)
Current				
DS 1	Oct 98	Sep 01	Borelly*	Rayman *et al.* (1998)
Stardust†	Feb 99	Jan 04	Wild 2	Brownlee *et al.* (1996)
Planned				
Rosetta	Jan 03	Jan 08	Wirtanen	Atzei *et al.* (1992)
Contour	Jul 02	Nov 03	Encke	Farquhar *et al.* (1997)
Contour	Jul 02	Jun 06	S-W 3	Farquhar *et al.* (1997)
Contour	Jul 02	Aug 08	d'Arrest	Farquhar *et al.* (1997)
DS 4	May 03	Dec 05	Tempel 1	Muirhead *et al.* (1997)

Abbreviations: G-Z = Giacobini-Zinner, G-S = Grigg-Skjellerup, S-W 3 = Schwassmann-Wachman 3.
*Extended mission only.
†Sample return January 2006.

The Nature of Comets

Comets are thought to have formed in the outer solar nebula in and beyond the giant planet region by agglomeration of interstellar grains (Greenberg, 1982), condensation, and accretion processes. The D/H ratios of Comets Halley, Hyakutake, and Hale-Bopp suggest an interstellar origin (see, *e.g.*, Vanysek, 1991). The combined gas and dust released from the nucleus of Halley's comet has solar abundances of O, C, and the nonvolatile elements, and is closer to solar abundance than CI chondrites for N, and may thus be

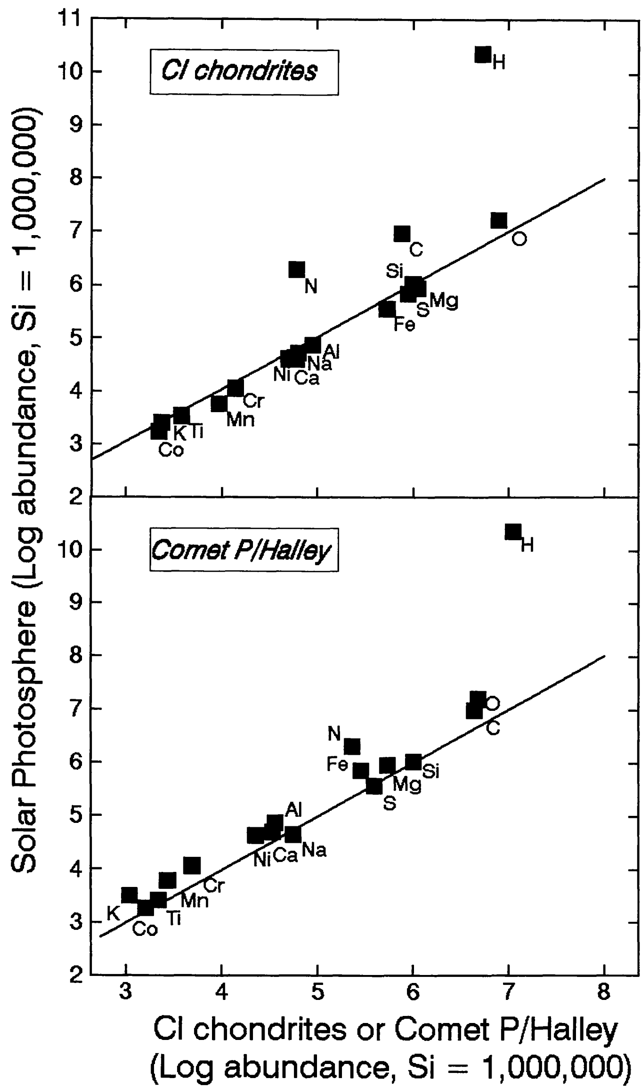

FIG. 1. Composition of dust from Comet P/Halley and CI chondrites compared with that of the solar photosphere (data from Ross and Aller, 1976; Jessberger *et al.*, 1988; Anders and Ebihara, 1982).

considered more primitive than chondritic meteorites (Fig. 1). Subsequent interaction with the major planets caused many to be ejected into a spherically symmetric cloud, the Oort cloud, 10^4 to 10^5 AU from the Sun, (Oort, 1950; Rickman and Huebner, 1990; Bailey *et al.*, 1986). Comets have also been found near the ecliptic 40 to 100 AU from the Sun ("the Kuiper Belt"); but in view of their faintness, only the largest nuclei have been detected (Jewitt and Luu, 1993; 1995). "The Centaurs" are a recently recognized group of comet nuclei in the outer solar system that are transitional between Kuiper Belt and short-period comets (Stern and Campins, 1996). The short-period comets (with a period <200 years) are either close to the ecliptic (the Jupiter family) or probably captured Oort cloud comets when out of the ecliptic (Halley family). Long-period comets have their origin in the Oort cloud, which has a diameter of about one light year, and have random directions.

Comparison of comet spectra with those of laboratory samples provides clues to the nature of the dust in comets (Fig. 2). Comet spectra contain bands at 9.2, 10.0, and 11.2 μm, with minor features at 10.5 and 11.9 μm. The 11.2 μm peak and 11.9 μm shoulder have been confidently attributed to crystalline olivine (Campins and Ryan, 1989; Hanner *et al.*, 1994a), whereas amorphous or glassy olivine is thought to explain the 10.0 μm feature. With less confidence, crystalline pyroxene probably explains the 10.5 μm feature and amorphous pyroxene the 9.32 μm feature (Stephen and

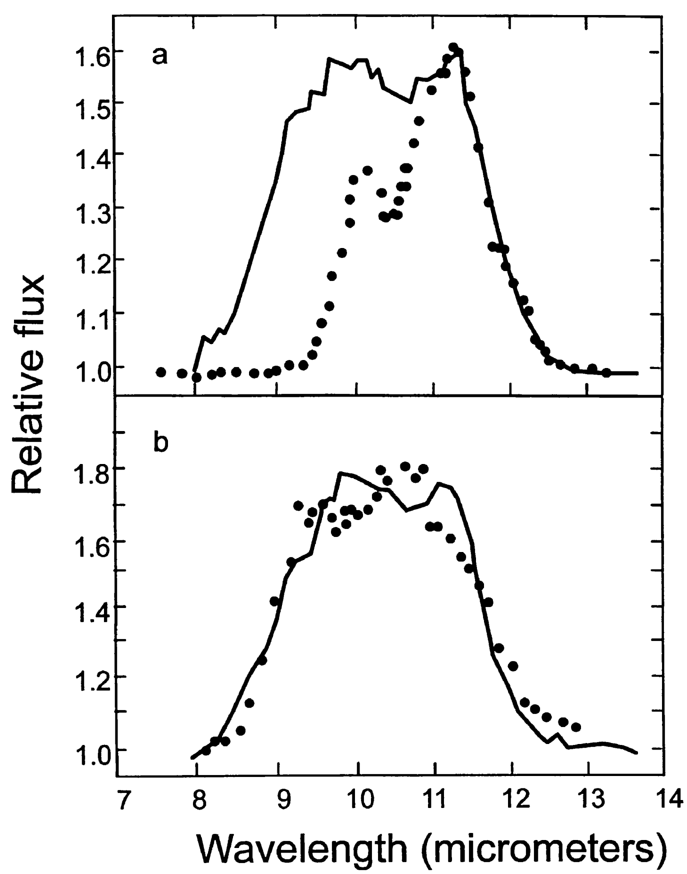

FIG. 2. Comparisons of the spectra of various solids measured in the laboratory with the spectra of comets. (a) The spectrum for ground olivine (filled symbols) compared with the spectrum for comet Halley (flux/continuum at r = 0.79 AU. (b) The spectrum for crystalline pyroxene (filled symbols) compared with the spectrum for comet Levy. (From Hanner *et al.*, 1994).

Russell, 1979). Bands at ~3.4 μm have been attributed to C-H stretch. Kolokova and Jockers (1997) derive the composition of the dust from polarization spectra.

Table 2 lists the neutral species present in the coma of comets as deduced from their spectra. This gives some indication of the volatiles emitted from the nucleus, although complex series of photolysis reactions occur in the coma and the coma has chemical abundances unlike the nucleus. Similarly, because of differences in the thermodynamic properties of the comet volatiles, it seems unlikely that the gases are released without chemical fractionation. Fractionation during trapping and detrapping of gases by crystalline matrices would further complicate the story. Despite this, it can be safely inferred that the ices in the nucleus are essentially water ice with small amounts of CO, CO_2, NH_3, some S, and organic compounds.

According to thermodynamic equilibria, crystalline water ice forms above ~135 K (Lewis and Prinn, 1980); but because of kinetic limitations, some authors suggest that amorphous ice, which has a remarkable ability to trap and retain gas, forms below ~135 K if the condensation flux is fast (Kouchi *et al.*, 1994). At reasonable black body temperatures for objects in the outer solar system, ~85 K, amorphous ice should be stable for several million years, the time-frame for the formation of the solar system (Klinger, 1980, 1991; Smoluchowski, 1981). However, others argue that formation of amorphous water ice requires an unreasonably high flux of water and sustained low temperatures (Kouchi *et al.*, 1994). Furthermore, crystalline ice has been observed in interstellar space surrounding the young main-sequence stars HD 100546 and HD 142527. The disk of HD 100546 shows polyaromatic hydrocarbons (PAHs), crystalline forsterite, some pyroxenes, amorphous olivine, FeO, and crystalline water ice (Kouchi *et al.*, 1994).

Much of our present observational data for the nucleus of comets resulted from spacecraft observations of Comet P/Halley (Fig. 3). The main results of the *Giotto* space mission to comet P/Halley were the low albedo of the nucleus (4%) (comparable to black velvet), its low gravitational field (about 5 × 10^{-5} times the Earth's), and the low density of the nucleus (0.3–0.5 g cm^{-3}) (see Table 8 below). The spacecraft also confirmed that H_2O was the main volatile component of the nucleus. Coma gas production could be explained with only ~20% of the sunlit surface of the nucleus being active, the remainder being covered with a dark mantle (Keller *et al.*, 1988). Gas and dust appear to be ejected from

TABLE 2. Neutral species directly observed in comets (A'Hearn and Festou, 1990) with recent additions for observations from comets Hyakutake and Hale-Bopp.*

Metals*	Other atoms	Diatomics	Triatomics	Polyatomics
Na	H	CH	H_2O	H_2CO
K	C	CO	CO_2	NH_3
Ca	N	CN	NH_2	CH_3CN
V	O	C_2	HCN	C_2H_2
Cr	S	CS	C_3	CH_4
Mn	–	OH	HCO	C_2H_6
Fe	–	NH	HNC	HNCO
Co	–	S_2	H_2S	H_2CS
Ni	–	$^{12}C^{13}C$	OCS	HC_3N
Cu	–	^{13}CN	SO_2	CH_3OH
–	–	N_2	–	NH_2CHO
–	–	SO	–	–

*Except for Na, metals are only observed in sun-grazing comets.

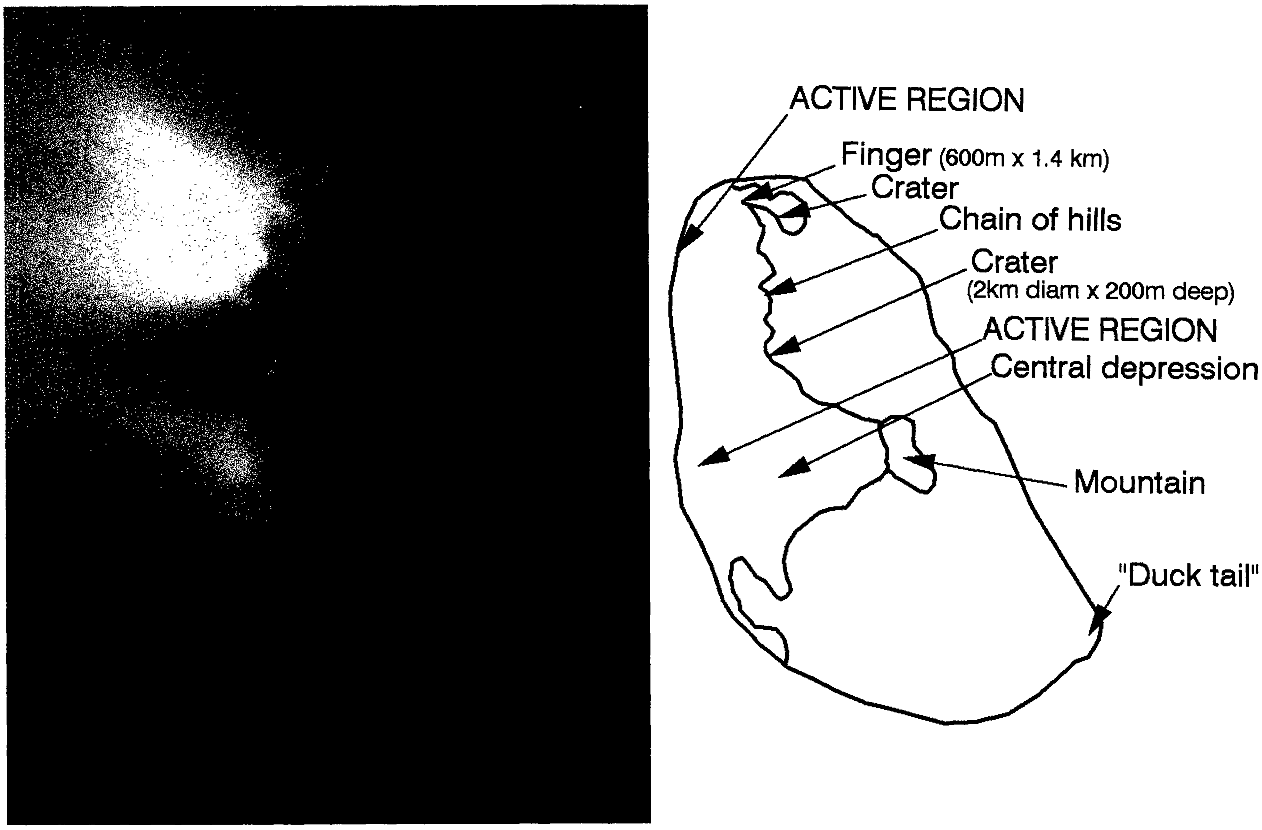

FIG. 3. The nucleus of P/Halley from the *Giotto* spacecraft made from six images taken 1986 March 13 at distances of 2730 to 14 420 km with a sketch showing the main features. One of the main observations of the Halley encounters was that the highly irregular nucleus is covered with a dark mantle, probably containing a number of active areas from which considerable degassing was occurring. (Image courtesy of H. U. Keller, Max-Planck-Institute für Aeronomie, Lindau/Harz, Germany. Sketch is from Keller, 1990.)

active areas; the dust to gas mass ratio is not well known but is probably ~2. The dominant gas (at least at 1 AU) is water vapor. The dust grains were a mixture of silicate grains with similar elemental abundances to carbonaceous chondrites and carbonaceous grains (hydrocarbon polycondensates) rich in C, H, O, and N (CHON) with some S (Jessberger *et al.*, 1988; Grün and Jessberger, 1990; Maas *et al.*, 1990; Krueger *et al.*, 1991). Huebner (1987) argued for the presence of polyoxymethylene in the surface materials of Comet Halley.

Evolution of Comet Nuclei and Their Surfaces

After the agglomeration of grains to form the comet nucleus, three stages of evolution can be identified. First, a short-lived initial formation stage (Fig. 4a). Second, residence in the Oort cloud or Kuiper Belt, which lasted most of the life time of the solar system (Fig. 4b). Third, deflection into the inner solar system, which is a relatively short-lived stage (Fig. 4c).

During the initial phase, there is the possibility of internal heating by ^{26}Al, although ^{26}Mg, the decay product, was not found in the *Giotto* data. Because of the very short half-life of ^{26}Al, it is very unlikely that it survived long enough to be incorporated in comet nuclei after its production in a supernova explosion. Silicates covered with ices probably formed a highly porous filamentary structure as a result of the low gravity field and the sublimation of volatiles, but there was probably also some impact-compaction. Thus the structures become fluffy but not fractal. Solar corpuscular radiation during the Sun's τ-Tauri phase may result in the loss and alteration of some volatile components by sputtering. There is also the possibility of impact between cometesimals that might alter their structure and composition.

During the long phase of residence in the Oort cloud, there is little alteration by solar heating because of the heliocentric distance from the Sun, but exposure to cosmic rays will probably produce an altered zone about a meter thick (Strazzula *et al.*, 1991). This is sometimes referred to as the "irradiation driven mantle." Irradiation by charged-particles is generally more important than sublimation in determining the nature of comet surfaces at distances >5 AU, although Comet Halley experienced an outburst in activity at 14 AU and Comets Bowell and Hale-Bopp had large comas when discovered at >6 AU. Individual interstellar grains could also have undergone irradiation prior to accretion onto the comets, as could grains ejected from the comet. Laboratory experiments suggest that this process will involve the release of gases and the formation of new organic compounds.

However, the most complex surface activity occurs during the passage of the comet nucleus through the inner solar system, when solar heating produces sublimation of volatiles, loss of gases, redistribution of heat in the subsurface layers of the nucleus, chemical fractionation, and the formation of complex strata of some recrystallized volatiles. These processes are described with references below. The amorphous ice of the interior is crystallized and a "sublimation driven mantle" (the refractory dust mantle) is produced on the surface. This eventually insulates the surface, increases surface temperatures and internal pressures, and reduces the

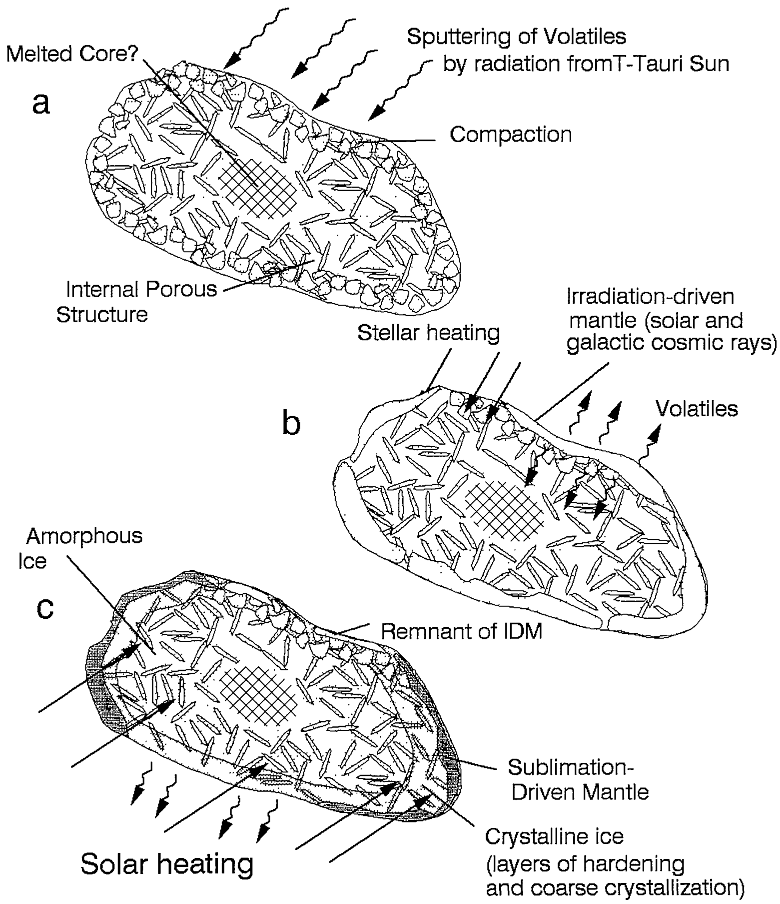

FIG. 4. Proposed interior structures of comets at the three major stages of their evolution. (a) Immediately following formation. (b) During storage in the Oort cloud. (c) During close approach to the Sun. (From Colangeli *et al.*, 1992b).

sublimation except for occasional outbursts when the mantle is disrupted. Thus there is an ageing process, so that comets new to the inner solar system will be more active whereas others will have their activity greatly reduced.

It was Whipple (1951) who first proposed that sublimation of volatile compounds would result in the formation of a refractory mantle on a comet nucleus as it entered the inner solar system. The general vision of a comet, consisting of a solid nucleus, being a mixture of water-ice and minerals ("dirty snowball") with a dark mantle, was convincingly demonstrated by the *Giotto* Space Mission to Comet P/Halley in 1986. Many authors have pursued Whipple's idea (Brin and Mendis, 1979; Shulman, 1972; Dobrovolsky and Kajmakow, 1977; Horanyi *et al.*, 1984; Dobrovolsky *et al.*, 1986; Prialnik and Bar-Nun, 1988). Fanale and Salvail (1984, 1986) produced a quantitative model for comet evolution and mantle formation, based on heat flux balance, gas transport, and mantle development. They also allowed for the effects of latitude, rotation, and spin axis orientation. They found that comets with a perihelion <1.5 AU will develop a mantle, especially after repeated passes through the inner solar system, although retention at small perihelia requires a cohesive force between the grains and nucleus. However, the high activity often observed requires that some exposed water ice or components more volatile than water (like CO_2, CO, or other frozen gases) should be present in the nucleus. Mantle formation of 1–3 cm resulted in irreversible changes to the comet and caused the H_2O flux to drop below 3×10^{12} molecules cm^{-2} s^{-1} (compared to a maximum of ~10^{18} molecules cm^{-2} s^{-1} at 1 AU). Fanale and Salvail (1986) also pointed out that if Apollo asteroids were extinct comets, they would have ice within ~10 cm of their surfaces. However, these results are based on one-dimensional models.

Kührt and Keller (1994) found that over a wide range of parameters the cohesion of the matrix material is stronger than the vapor pressure building up underneath the mantle. These conditions lead to stable mantles and do not explain all the activity of comet nuclei. In the KOSI 9 experiment, the dust mantle was partially removed by an avalanche and the bare ice/mineral-matrix was exposed to solar radiation (Grün *et al.*,1993). Möhlmann (1995) describes the formation of a regolith layer, consisting of particles in the centimeter and decimeter range, that can fall down after lift-off and can be deposited at inactive parts of the comet surface. The heating effects associated with passage through the inner solar system will be superimposed on the earlier irradiation produced mantle.

The surface of a short-period comet in the inner solar system has a complex layered structure. On the surface is the dust mantle. Below this, there are harder, recrystallized layers corresponding to each of the major volatile components that were observed in the early KOSI experiments (see below). When this is modeled as a bundle of roughly parallel cylindrical channels, it is found that the gas flow rate varies with pore length/radius ratio (Skorov and Rickman, 1995). Small-scale structures in the surface layer probably determine how the activity develops; the erosion of ice-filled channels embedded in a matrix composed of nonvolatile material is limited by the gas recondensating at the bottom (Benkhoff and Spohn, 1991; Markiewicz *et al.*, 1998). There might conceivably be gas-filled voids and regions of disrupted mantle where vents may release gas and dust to space or where ice may be exposed (Fig. 5). The ability of the gases to eject dust, or even lift-off larger silicate- or ice-particles, depends on the distance from the Sun. Depending on the size of the comet nucleus, the drag coefficient, and area-to-mass ratio, there could be up to meter-sized boulders strewn on the surface that were ejected and have fallen back.

Comets are highly irregular in shape and might show considerable surface relief (Fig. 6). There might also be craters, from which gases and their entrained dust particles are expelled. Much of the material that leaves the surface with any velocity would be lost to space, with only the larger and denser particles landing elsewhere on the surface to add to the dust mantle.

Most recently the observed comets were heated by passage through inner solar system. The spectacular naked-eye comets are usually long-period comets ($P < 10^6$ years) that have not made multiple passes through the inner solar system. The details of how a comet nucleus behaves in the inner solar system depend on many factors. Some of these are global heat flow, the redistribution of volatile compounds and their latent heat, possibly hydrate formation, changes in porosity and the relative amounts of the several forms of crystalline and amorphous ice, and the presence and nature of internal heat sources (Rickman, 1991).

Thus comets "age" as they make repeated passes through the inner solar system; and as they do, the dust mantle builds up, suppressing sublimation through increased thermal emission. It seems that the increased IR radiation into space (caused by mantle

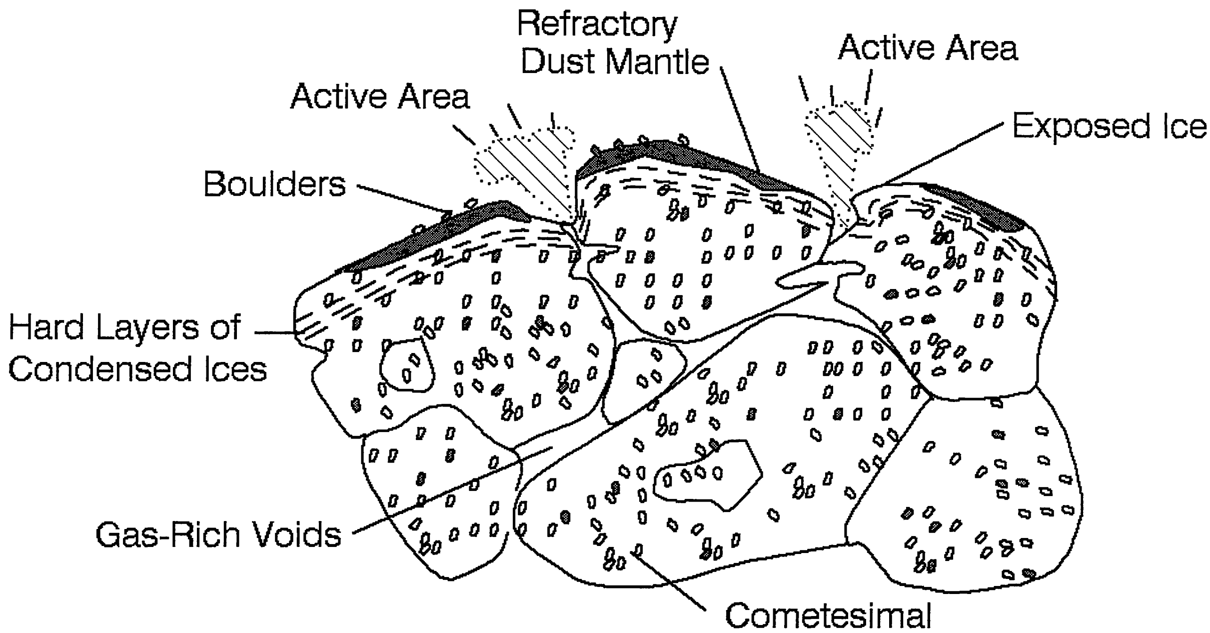

FIG. 5. Proposed structures for a comet regolith, although it is doubtful that they would all occur at any particular landing site. (From Stöffler and Düren, 1992).

development that deprives the comet nucleus of heat for sublimation) reduces its activity and brings a comet's life to an end, rather than the exhaustion of volatiles. Therefore many of the Amor-Apollo asteroids may be extinct comets (Rickman and Huebner, 1990).

Models for Comet Nuclei

Whipple's (1950) view that comet nuclei are essentially icy conglomerates (Fig. 7a) has been augmented by a number of models involving large amounts of dust (Donn, 1991; Colangeli *et al.*, 1989, 1992a). It might be more appropriate to think of comets as "icy dustballs," rather than "dirty snowballs," with a predominant refractory component (Keller, 1989). Öpik (1971) has suggested a rubble-pile structure (Fig. 7b), which was revived by Weissman (1986), whereas Gombosi and Houpis (1986) suggested a structure consisting of silicate grains cemented by ices, an "icy-glue model" (Fig. 7c). Donn and Hughes (1986) have suggested that the nucleus is a random assemblage of ice-coated silicate grains with a fluffy (sometimes called "fractal") structure (Fig. 7d). Möhlmann (1995) has suggested that the nucleus consists of a cohesively bound matrix of refractory and porous matter with water ice in the pores and activity restricted to impact-produced "debris-zones" between the original "cometesimals." Flow of volatiles throughout the nucleus towards this region of activity would ultimately lead to global planes of weakness and the nucleus might split. Comets are observed to split in half with a frequency of about one per 100 years (Möhlmann, 1996). This theoretical number is probably low, and Sekinina (1997) lists 25 split comets not totally disrupted and several that were totally disrupted by Jupiter are now known.

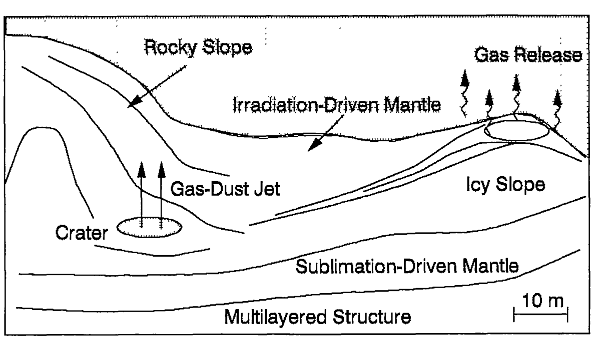

FIG. 6. A possible comet landscape as deduced from comet simulation experiments, astronomical observations, and theoretical considerations (Colangeli *et al.* 1992a).

Comet Simulation Experiments: Some General Considerations

Most scientific investigations of Nature make some use of laboratory studies, whether it is examining a mountain through a microscope or exploring the formation of continents through experimental petrology and thermodynamics. Clearly one cannot reproduce a comet, with a 10 km nucleus and 10^8 km tail, in the laboratory. Similarly, the method of producing the comet analogue materials predetermines their properties to some extent. Clearly the limitations of these experiments and their applicability to real comets must be borne in mind. However, physical laws are independent of location so it should be possible to understand at least some of the effects through laboratory experiments, even if the complete environment cannot be reproduced. Thus whereas small-scale experiments provide information on the basic physics and chemistry of low-temperature ice-dust-gas samples, large-scale experiments give information in the tens of centimeter scale.

The most fundamental differences between real and simulated comet nuclei are their mass and size, which are known approximately but not reproducible in the laboratory, and the identity and composition of all the constituents of comet nuclei, these being reproducible but poorly known. Processes occurring in the comet on the kilometer scale must be reproduced in the laboratory on the decimeter scale. In the protoplanetary disk, dust grains accumulated into ever-growing aggregates while volatile compounds are trapped into them. It is difficult to impossible to produce large comet analogues under microgravity conditions and by condensation from a gas-phase or by crystallization. Microgravity cannot be simulated easily on Earth for more than a few minutes. The production of comet

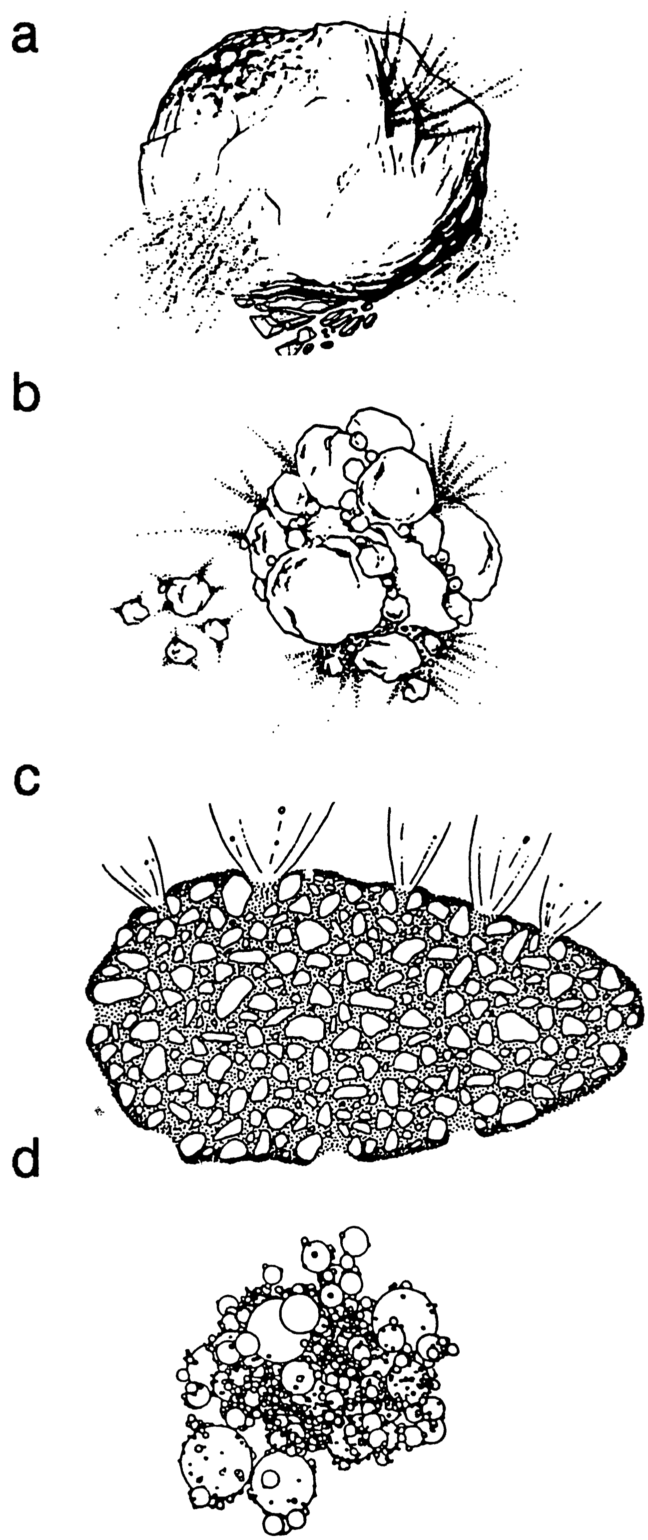

FIG. 7. Sketches showing four currently popular views of the interior structures of comets. (a) Icy conglomerate model of Whipple (1950), drawing from Weissman and Kieffer (1981). (b) Öpik's (1971) rubble pile model as revived by Weissman (1986). (c) The icy-glue model of Gombosi and Houpis (1986). (d) The fluffy ("fractal") model of Donn and Hughes (1986).

analogues by spraying aqueous suspensions of micrometer-sized minerals into liquid nitrogen is a crude approximation to condensation and crystallization from a gas phase. For example, one might expect amorphous ice to form under interplanetary conditions, whereas spraying produces hexagonal ice. One major difference in these two forms of ice is the high gas-trapping capabilities of amorphous ice, the gases being released as the ice undergoes phase changes.

Comet simulation experiments played an important role in clarifying processes of devolatilization of surface layers of comet nuclei and helped in the formulation and realization of the existence of a third source for coma gases. Thus three sources for coma gases exist: (1) the surface of the nucleus (releasing mostly water vapor), (2) the dust in the coma (the distributed source of several species released from dust particles), and (3) the interior of the porous nucleus (the source of many species more volatile than water). The species diffusing from the interior of the nucleus are released by heat transported into the interior. Thus, the ratio of volatile compounds relative to water in the coma is a function of the heliocentric distance and provides important information about the chemical composition and structure of the nucleus.

LABORATORY EXPERIMENTS

Production of Comet Analogue Materials

The first comet simulation experiments were performed as early as 1967 by Russian groups in Dushanbe (Ibadinov and Kajmakov, 1970) in the former Tadjik Socialist Soviet Republic, and in St. Petersburg, the former Leningrad (Kajmakov and Sharkov, 1967). Small samples of water ice and sand, deposited from vapor mixtures on a cold finger, were exposed to a strong light source. Procedures involving thin films were also used by Greenberg (1977, 1982, 1986) and Strazzulla *et al.* (1983). The method is represented by the sketch in Fig. 8a.

For large samples, other methods have to be used. Saunders *et al.* (1986) sprayed slurries of water and clay minerals into liquid nitrogen using N_2 at 500 psi (3.4 Gpa) (Fig. 8b). Several Russian groups have used the same procedure (Kajmakov and Sharkov, 1967; Ibadinov and Kajmakov, 1970; Dobrovolsky *et al.*, 1986). Kochan *et al.* (1989a,b), Grün *et al.* (1991a,c, 1992), Kochan and Junglus (1993) and Seidensticker and Kochan (1992) used a large-scale automated version of this method to produce 30–60 cm diameter comet analogues with a depth of 14–30 cm for the KOSI experiments. Clay minerals are used, along with some olivine, as the silicate dust in the comet simulation experiments. Organic compounds and suspended graphite provide the C species and the low albedo ("blackness") of the simulated comet material. Oehler and Neukum (1991) found that the albedo of the samples was 10–18% for the KOSI 3, 4, and 6 experiments (see Table 3). Kilogram-quantities of an aqueous suspension of phyllosilicate (kaolinite, <2 μm particles, or montmorillonite, <35 μm particles) and nesosilicates (olivine or dunite, 4–8 μm particles), and C (0.85 nm particles) were sprayed into liquid nitrogen, sometimes with other components such as CO_2 or methanol. The various mixtures used are listed in Table 3, a schematic of the apparatus is shown in Fig. 8c, and photographs showing the apparatus and final product are shown in Fig. 8d,e.

Sample production at very low temperatures from the gas phase should result in amorphous ice. Production of thin amorphous, gas-laden, ice was demonstrated by Bar-Nun and others in many papers (*e.g.*, Bar-Nun *et al.*, 1985). The production of thick samples is troublesome but is currently achievable (Bar-Nun, pers. comm.).

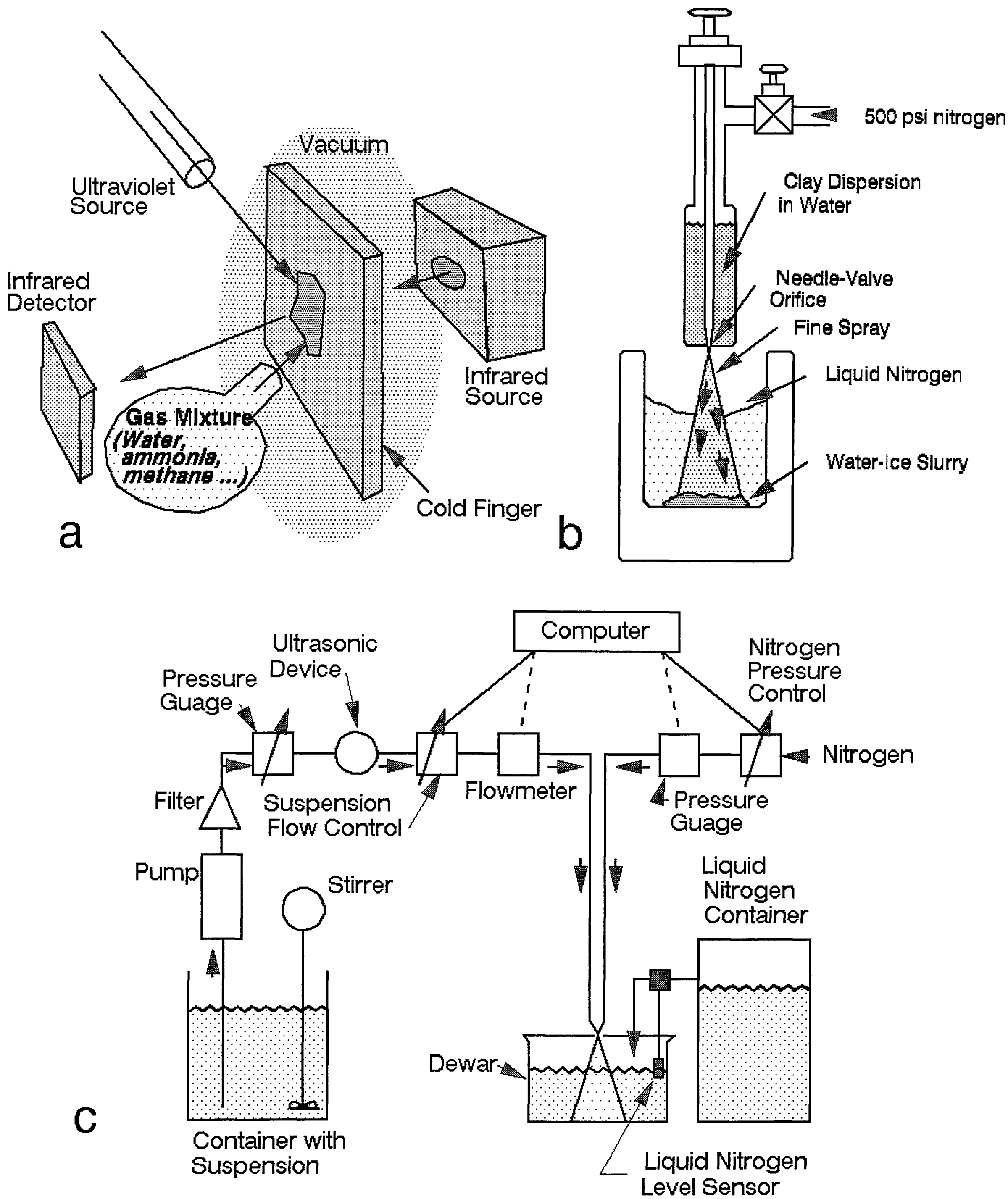

FIG. 8. (above and right) Various techniques for producing comet analogue material. (a) Greenberg's (1982) method for producing thin films for solar spectrum irradiation and IR spectroscopic investigation. (b) The Saunders *et al.* (1986) method for producing silicate residue structures. (c) Schematic diagram for the apparatus used to produce experimental analogues of comet material for the large-scale KOSI experiments (Stöffler and Düren, 1992).

Bar-Nun (1991) attempted such sample preparation by depositing a 1:1 mixture of $CO:H_2O$ on a cold finger at 48 K and a 1:10 mixture of $CO_2:H_2O$ at 70 K. Large-scale production of gas-laden amorphous ice with an admixture of mineral dust is highly desirable, but the procedures are technically challenging. Either a lock has to be installed between the production machine and the experimental sample container, or the production of the sample has to take place directly in the experiment container. An environmental temperature of ~100 K is required.

Small-scale Comet Simulation Experiments

Greenberg's measurements were made in the apparatus in which the analogues were made (Fig. 8a; Greenberg, 1977, 1982, 1986). Examples of other small-scale apparatus for the study of comet

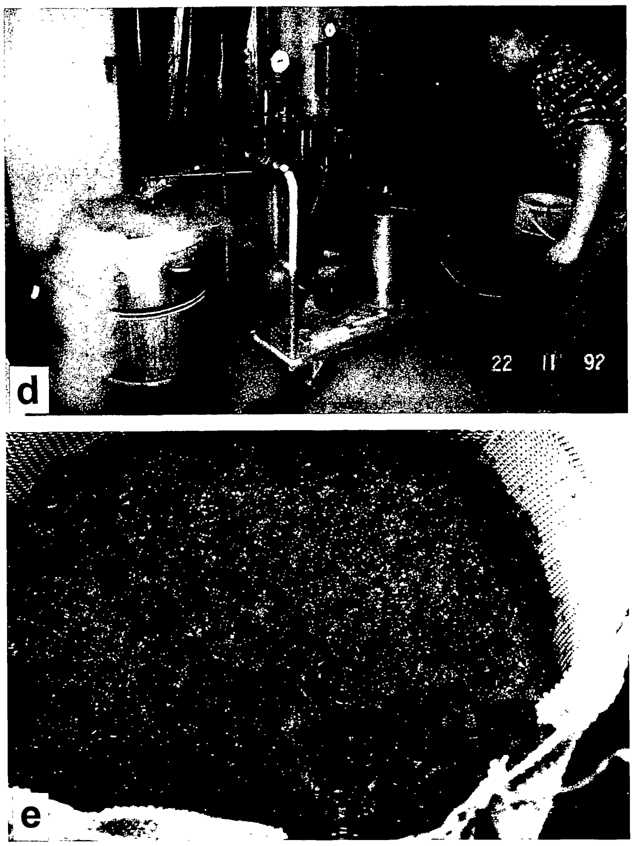

FIG. 8. *(continued)* (d) A photograph of the apparatus described in (c) during the preparation of a sample. The spray gun is on the right and the mixer is on the left. (e) The appearance of the analogue material prior to placement in the KOSI apparatus.

analogues are shown in Fig. 9. A series of similar experiments has also been summarized by Dobrovolsky *et al.* (1986), Ibadinov and Aliev (1987), and by Ibadinov *et al.* (1991) whose apparatus is shown in Fig. 9a. Comet analogues typically of H_2O-ice with admixtures of graphite, quartz, or nickel particles (1–30 μm) were irradiated with Xe lamps at 10^{-4} Pa at 80 K (Fig. 9a). Seidensticker and Kochan (1992) describe a small chamber at the DLR (Fig. 9b) of a 60 cm diameter × 64 cm height that could be evacuated to 0.1 torr and expose 10 × 10 cm samples to the equivalent of 2 solar constants irradiance from Xe lamps. Table 4 shows the relevant parameters of this chamber.

Figure 9c shows Seidensticker and Kochan's (1992) small-simulation chamber with the oil-diffusion pump below, video camera, and the liquid nitrogen inlets at the top, and the Xe high-pressure lamp and a video recorder with screen to the right. Figure 9d shows the internal instrumentation, mounted below the cover, hoisted above the chamber prior to assembly. The instrumentation consists mainly of the cold shroud with the sample container at the center of the assembly and with a hardness tester just above the container. The hardness tester is operated *via* a vacuum feed-through, so that the sample can be monitored during the experiment. The sample container, standing on a liquid nitrogen-cooled Cu prism, is tilted 45° to the horizontal so that the space in front of the sample can be viewed through a window by a video camera and the surface and dust emissions can be monitored.

More specialized equipment was used by Rössler *et al.* (1992a) to explore the effect of vacuum UV on comet analogues (Fig. 9e). Strazzula *et al.* (1983) have used small-scale simulation experiments to investigate the modification to the surfaces of thin films of condensed gases by ionizing radiation (Fig. 9f). Ions of H, He, and heavier nuclei were generated in the 10–100 keV energy range by a van der Graff generator. The operating pressure and temperature range were $<2 \times 10^{-7}$ torr at 4–200 K, respectively. Johnson *et al.* (1987) used similar apparatus, and the whole subject of energetic charged-particle interactions with atmospheres and surfaces was recently reviewed by Johnson (1990) and Strazulla and Johnson (1991). Bar-Nun *et al.* (1985) investigated the trapping and release of H_2, CO, CO_2, CH_4, Ar, Ne, and N_2 by amorphous water ice at 16 K and $5 \times (10^{-8}–10^{-6})$ torr using the apparatus in Fig. 9g,h. Recently Kömle *et al.* (1996) have constructed apparatus to explore the effect of mantles of different albedos and porosities on the thermal behavior of comet nuclei.

Large-scale Comet Simulation Experiments

The largest and most ambitious comet simulation studies to date are the so-called "KOSI" (Kometen-Simulation) experiments performed at the DLR in Cologne (Kochan *et al.*, 1989a,b; Thiel *et al.*, 1989; Grün *et al.,* 1987, 1991a, 1992; Seidensticker and Kochan, 1992; Kochan and Junglus, 1993). The large DLR Space Simulator, designed initially to test space hardware, is a 4.9 m long, 2.5 m diameter cylinder inside a cold shroud that can be evacuated to a pressure of 10^{-6} Pa. The apparatus is shown in Fig. 10 and described in Table 5. Eleven experiments were performed between 1986 and 1993 (Table 3).

The Cu sample container (30–60 cm diameter and 15–30 cm deep, see above) is cooled by liquid nitrogen flowing through the back plate. The cooling system is independent of the rest of the comet simulator and can be moved with the sample. A glove box is used for a variety of studies after removal of the samples from the chamber. These include optical inspection of the surface and interior, photography, and measurement of hardness.

Ten Xe lamps with an approximately solar spectrum provide ~2.3 kW power over an area 1.3 m in diameter (equivalent to ~1.25 solar constants). The chamber also contains ionization gauges, a quadrapole mass spectrometer, several hundred dust detectors, ten piezo electric detectors, television cameras, and an infrared photometer.

The emitted ice and dust particles were collected during the insolation by ~200 small boxes arranged in an array of heated rails (Fig. 10c). The heated rails ensured that the boxes and samples remained dry during warmup. To monitor the time variation of the particle emission, some of the collectors had rotating carousels that enabled them to be opened in a stepwise fashion (Thiel *et al.*, 1995). The dust particles were subsequently examined by optical and scanning electron microscopy (Thiel *et al.*, 1995).

OBSERVATIONS DURING LABORATORY EXPERIMENTS

The main themes we will discuss in the following section are the physical phenomena observed *in situ* during the experiments, such as the particle emission, the thermal history and modifications to the bulk sample, and then observations of the surface and interior of the sample after removal from the simulator. However, first we will review experiments on radiation effects, because these are the major comet surface alteration processes prior to the comet entering the inner solar system.

Radiation Effects on Comet Material

The effects on comet analogues of charged-particle irradiation have been investigated by Strazzula and Johnson (1991) and

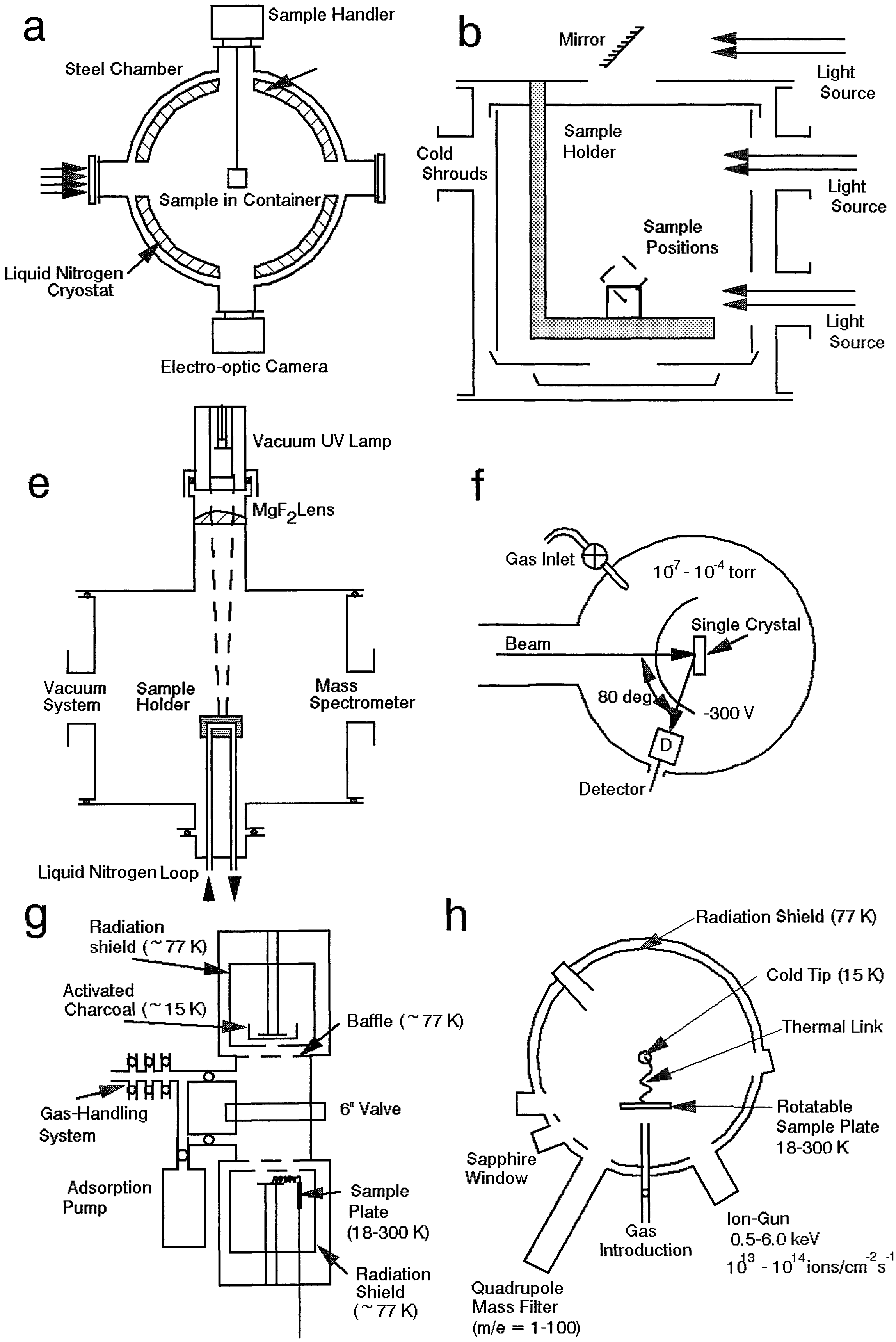
a
Sample Handler
Steel Chamber
Sample in Container
Liquid Nitrogen Cryostat
Electro-optic Camera
b
Mirror
Light Source
Cold Shrouds
Sample Holder
Light Source
Sample Positions
Light Source
e
Vacuum UV Lamp
MgF_2 Lens
Vacuum System
Sample Holder
Mass Spectrometer
Liquid Nitrogen Loop
f
Gas Inlet
10^{-7} - 10^{-4} torr
Single Crystal
Beam
80 deg
-300 V
D
Detector
g
Radiation shield (~77 K)
Activated Charcoal (~15 K)
Baffle (~77 K)
6" Valve
Gas-Handling System
Adsorption Pump
Sample Plate (18-300 K)
Radiation Shield (~77 K)
h
Radiation Shield (77 K)
Cold Tip (15 K)
Thermal Link
Rotatable Sample Plate 18-300 K
Sapphire Window
Gas Introduction
Ion-Gun 0.5-6.0 keV
10^{13} - 10^{14} ions/cm^{-2}s^{-1}
Quadrupole Mass Filter (m/e = 1-100)

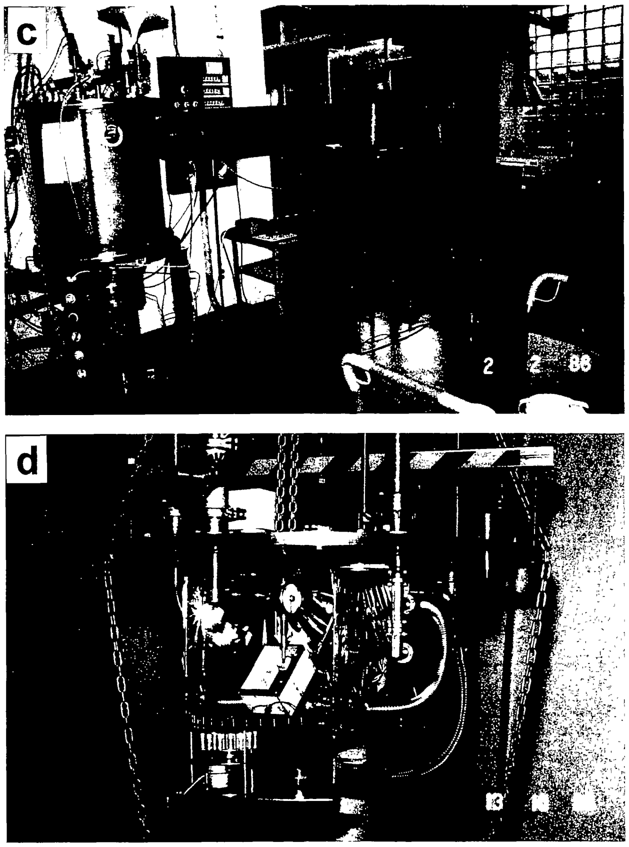

FIG. 9. (left and above) Various designs of apparatus for comet simulation experiments. (a) Ibadinov *et al.* (1991) for solar spectrum irradiation. (b) Seidensticker and Kochan (1992) for solar spectrum irradiation. (c) Photograph of the apparatus shown in Fig. 9b. The chamber is the 65 cm tall, 60 cm diameter cyllinder on the left with an oil diffusion pump underneath. The high-pressure Xe lamp is on the right, a video recorder and screen are on the far right of the photograph. (d) Apparatus rig before being lowered into the small chamber (Fig. 9c). The white box in the center of the rig houses the sample that has a hardness tester just placed above it. (e) Rössler *et al.* (1992a) apparatus for vacuum UV (<200 nm) irradiation. (f) Strazzula *et al.* (1991) apparatus for energetic charged particle irradiation. (g) Bar-Nun *et al.* (1995) apparatus for experiments exploring gas-trapping by amorphous ice, side elevation. (h) Horizontal section of the lower half of Fig. 9e showing the arrangement of the sample and instrumentation.

Strazzula *et al.* (1983, 1991). Sputtering by energetic solar wind particles results in the release of a number of neutral species (Table 6) and the build-up of a refractory mantle. Table 7 shows Strazzulla and Johnson's (1991) results for a methane ice target. Strazzulla *et al.* (1991) argue that even water-rich comets would acquire a carbonaceous mantle a few meters thick that would survive several passages through the inner solar system. Thus a spacecraft attempting to sample primordial comet material might have many meters of mantle to penetrate.

Gas, Dust, and Mantle Formation during Insolation

Gas Emission Activity–As expected, the gas flux produced during the KOSI experiments generally correlates with the intensity of irradiation, assuming there are no phase transformations in the ices (Grün *et al.*, 1993; Fig. 11). The decrease in the flux from 10^{18} molecules cm^{-2} s^{-1} is presumably in part related to dust mantle build-up. Figure 12 shows the H_2O and CO_2 release for a typical KOSI experiment (KOSI 3, with a H_2O-to-CO_2 weight ratio of 5.6:1). Water release rates decrease from ~10^{18} to ~10^{16} molecules cm^{-2} s^{-1}, whereas CO_2 release rates decrease from ~10^{17} to ~10^{16} molecules cm^{-2} s^{-1} during the 50 h duration of the experiment. The H_2O and CO_2 released during KOSI irradiation of samples and measured by mass spectroscopy had release rates of 10^{18} molecules cm^{-2} s^{-1} which is consistent with theoretical predictions (Huebner, 1965).

Hesselbarth *et al.* (1991) measured gas fluxes and compositions using pressure gauges and a quadrapole mass spectrometer ~1 m from the surface of the KOSI 4 experiments (H_2O-to-CO_2 weight ratio of 5:1, corresponding to a molar ratio of ~7.8:1). Fluxes were ~10^{17} to 10^{16} molecules cm^{-2} s^{-1} with CO_2 fluxes being a factor of ~2 below H_2O fluxes. The CO_2 and H_2O are released separately, CO_2 subliming at lower temperatures (~125 K) from deeper sample layers than H_2O (~200 K). The difference in release temperatures for CO_2 and H_2O presumably reflects both vapor pressure differences and differences in interactions with the matrix. One might expect that there would be an initial pulse of gases high in CO_2. This was not mentioned by Hesselbarth *et al.* (1991), although there was an initial pulse in the third period of exposure during the KOSI 9 experiment (Fig. 11). When illumination reaches one solar constant, H_2O and CO_2 release rates increased rapidly and then more slowly, the H_2O release slowing down faster than the CO_2 release rate.

Bar-Nun *et al.* (1985) measured the release of H_2, CO, CO_2, CH_4, Ar, Ne, and N_2 from amorphous water ice using the apparatus shown in Fig. 9g,h. The CO, CH_4, Ar, and N_2 were released in four temperature intervals corresponding to release mechanism and phase changes in the ice. Between 30 and 59 K, straight evaporation occurred; over the temperature ranges 135–155, 165–190, and 160–175 K, gas release was associated with conversion of amorphous to cubic ice, breakdown of trapping of volatiles, and conversion of cubic to hexagonal ice, respectively. Neon was not trapped by the ices.

Formation of the Mantle and Dust Emission Activity–A final dry dust mantle produced in the KOSI experiments was usually a few millimeters thick (Grün *et al.*, 1993). It took about an hour to fully form but the process was strongly temperature-dependent and could be described by the relationship:

$$f = 1 - (1 - f_0)\exp(-t/\tau) \tag{1}$$

in which f is the fraction of the surface covered at time t and f_0 is the fraction of the surface covered initially. The term τ is a characteristic time scale for the process that is given by:

$$\tau = (32\,\pi\,k\,T_i/9\,\mu)^{1/2}\,(\rho_d/P_s)((1 - v_s)/v_s)\,s \tag{2}$$

where k is Boltzmann's Constant, μ is the mass of a water molecule (3×10^{-26} kg), ρ_d is the particle density, P_s is the saturation vapor pressure, T_i is the ice temperature, v_s is the mass fraction of dust in the sample, and s is the mean radius of a spherical dust grain being ejected. Kömle *et al.* (1991) also simulated a nonvolatile, sintered crust formation on comets and found that the crust resulted in high temperatures and pressures (several Pa). However, it is unlikely that these results simulate the porosity of the actual mantles.

Kölzer *et al.* (1995) reported temporal variation in emission events of KOSI 5. Mass, size, density, trajectories, and drag equations for transfer of momentum from gas to dust were determined and source locations measured. They concluded that surface development has two steps: formation of dry particles and an associated build-up of the mantle.

Kochan and Koerver (1991) and Kochan *et al.* (1991) placed CCD-video cameras equipped with macro lenses over comet analogues in the small DLR chamber (Fig. 13). They measured particles of a few millimeters in size and final velocities of a few meters per

TABLE 3. The KOSI comet simulation experiments.*

	KOSI experiment number										
	1	2	3	4	5	6	7	8	9	10	11
Sample composition											
H_2O	90	90	78	77	70†	42†	83‡	100	90	90	45
CO_2	–	–	14	15	17†	15†	15‡	–	–	–	5.8
Others	–	–	–	–	MeOH 4%	–	–	–	–		9.1§
Dust	10	10	8	8	9	43	2	–	10	10	40
D/I$^{\#}$	0.11	0.11	0.09	0.09	0.01	0.75	0.02	0	0.11	0.11	0.67
Dust composition											
Olivine	–	90	90	90	89	71	91	–	100	100	50
Mont	–	10	10	10	11	17	–	–	–	–	50
Carbon	1	0.1	0.1	0.1	1.0	12	1	–	–	0.1	–
Kaol	99	–	–	–	–	–	–	–	–	–	–
Kerogen	–	–	–	–	–	–	8	–	–	–	–
Initial sample properties											
Albedo	0.2	0.06	0.17	0.07	0.08	0.12	0.07	0.9	0.061‡	n.d.	0.56
Density	0.4	0.6	0.5	0.5	0.56	0.59	0.46	0.40	0.44	0.50	0.54
Porosity	60	40	50	50	40	29	45	56	53	49%	49%
R_o	29	29	29	29	29	69	29	–	13.0	–	–
R_f	15	14	13	13	13	29	12	–	12.2	–	–
Irradiation											
Flux range	0.15	0.9	1.4	0.65	1.2	1.2	1.0	1.0	1.4	1.0	1.3
	–1.15	–	–	–0.85	–1.0	–1.4	–	–	–0.15	–0.6	–0.5
Duration	38.4	39.4	47.2	44.5	12.9	30.3	34.0	40.0	59.0	4.75	15.25

Details of the composition of the comet analogue material and some physical properties and conditions of the experiments (Seidensticker and Kochan, 1992; Grün *et al.*, 1993).
*Abbreviations and units: compositions (wt%); Kaol = Kaolinite; Mont = Montmorillonite; density (g cm^{-3}); porosity (%); duration (h, including dark periods); typical flux (solar constants, 1.37 kW m^{-2}). R_o = inital sample thickness (cm); R_f = final sample thickness (cm); MeOH = methanol.
‡Isotopically labelled.
†Albedo after the experiment was 0.122.
§6% formaldehyde, 2% methanol, 0.7% ammonia, and 0.4% heavy water.
$^{\#}$Dust-to-ice weight ratio.

second. The images show ice–dust agglomerates covered with ice. This ice might act as "cement" between grains. Grains do not erupt from the surface, but gas flow breaks up agglomerates until drag exceeds gravity and particles lift off slowly (a few centimeters per second). The failure stress estimated from the angle at which avalanches occur on the surface is very low, ~10 Pa (Grün *et al.*, 1993). An important discovery was that the dust particles were connected to the ice–mineral matrix by "sinter necks." The upstreaming gas from the sublimation of the volatiles inside the sample first erodes the sinter necks, and then the particles can entrain into the gas jet and are lifted-off.

TABLE 4. System parameters for the small comet simulation chamber at DLR.

Cold Shroud	
Form	vertical cylinder
Diameter	0.60 m
Height	0.64 m
Volume	0.2 m^3
Temperature	80 K (liquid nitrogen-cooling)
Samples	
Diameter	0.10 m
Height	0.10 m
Vacuum system	prepump + oil diffusion pump
Pressure	10^{-3} Pa
Light Source	
Bulb	1 × 6.5 kW Xe high pressure
Insolation intensity	2 Solar Constant (1 SC = 1.37 kW m^{-2})

TABLE 5. Data for the KOSI Space Simulator at the DLR.

Chamber	
Form	horizontal cylinder
Cold Shroud	
Diameter × length	2.5 × 5.1 m
Volume	25 m^3
Absorptivity/emissivity	0.90/0.92
Experiment Support Structure	
Width × height × length	1.7 × 1.7 × 5.0 m
Vacuum System	
Effective Pumping Capacity	3 × 15.000 L/s
Final Pressure	10^{-6} Pa
Cooling System	
Cooling liquid	liquid nitrogen
Cooling time	~30 min
Time for warming up	4 h
Solar simulator	
System	divergent beam (half angle 4°)
Radiation source	Ten 6.5 kW Xe high-pressure bulbs
Beam diameter at sample position	0.7 m
Irradiance (maximum)	2 solar constants (3 kW/m^2)

TABLE 6. Erosion yields from the bombardment of icy targets by 1.5 MeV He ions (Strazzula and Johnson, 1991).

Target	Yield*	T(K)	Released neutral species
H_2O	8	10–77	H_2, O_2, H_2O
CO_2	120	10	CO, CO_2, O_2
CH_4	100	10	H_2, C_2H_2, CH_4
NH_3	140	10	H_2, N_2, NH_3, N_2H_4
SO_2	16	10–77	O_2, SO, SO_2, SO_3
S_8	10	77–200	S_2

*Molecules released per bombarding ion.

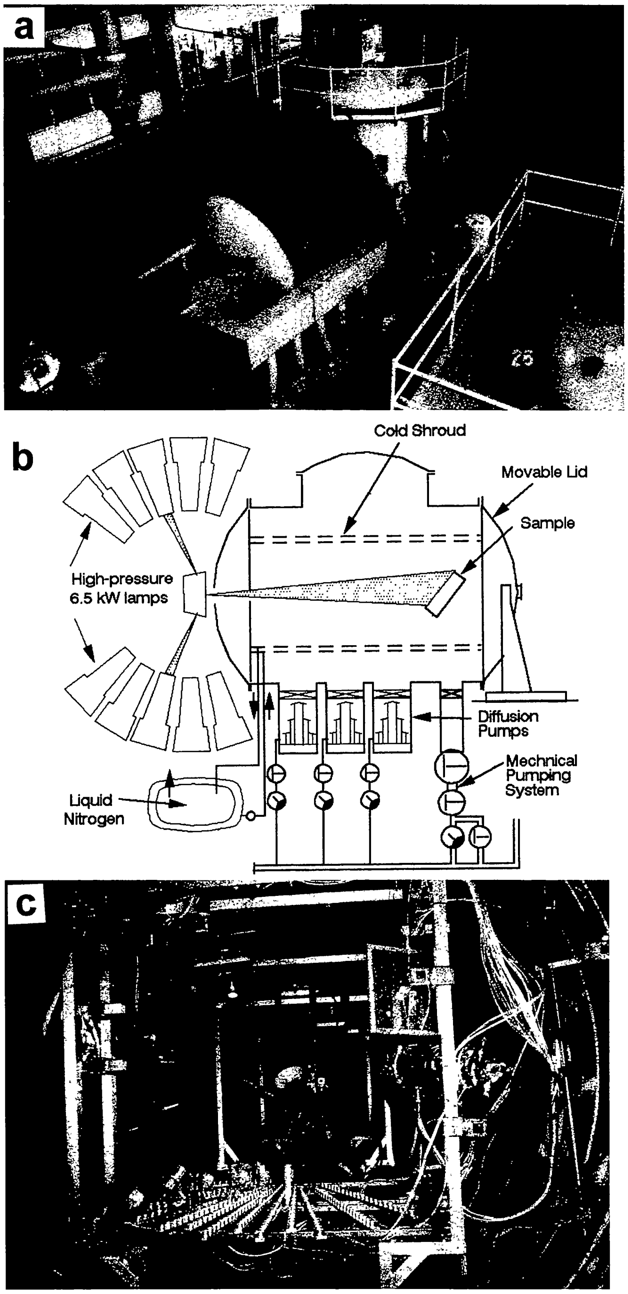

FIG. 10. (a) The DLR space simulator used for comet simulation experiments in an opened position. The cold shroud housing the comet analogue is located inside the chamber. The instrument rack can be seen just inside the cold shroud (Kochan *et al.*, 1989a). (b) Schematic diagram of the apparatus (Seidensticker and Kochan, 1992). (c) Photograph of the experimental rack placed opposite the comet analogue in the KOSI apparatus.

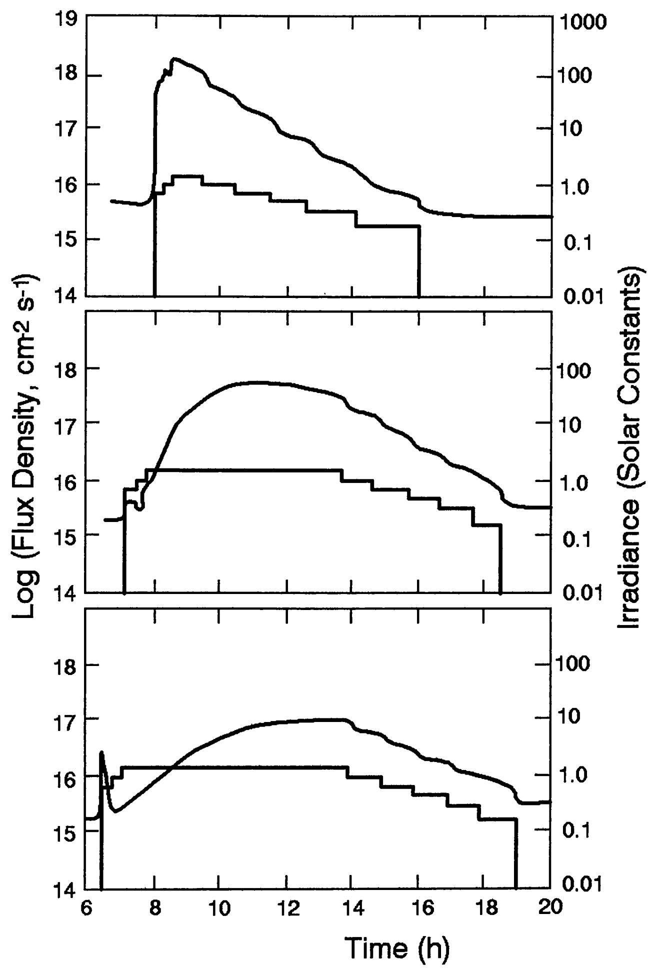

FIG. 11. Gas flux (continuous curves with scales on the left) compared with irradiance (stepped curves with scales on the right) during three periods of illumination of a comet analogue. (KOSI 9 experiment, Grün *et al.*, 1993).

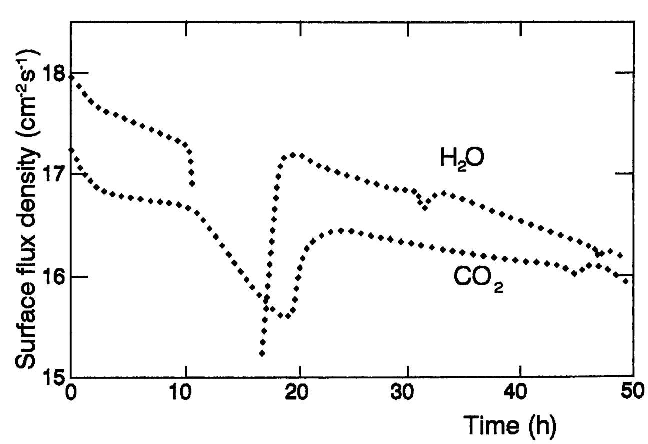

FIG. 12. Flux of water and carbon dioxide from the surface of the KOSI 3 sample as a function of the time from the beginning of the experiment. The discontinuity at 10–18 h reflects an interuption to the exposure (Grün *et al.*, 1991c).

TABLE 7. Properties of the mantle produced by MeV proton bombardment of frozen methane at 10 K (Strazzula and Johnson, 1991).

Fluence (H^+/cm^2)	Energy (eV/mol)	C/H Initial	C/H Heated*	Resulting material	Color	Bulk density ($g\ cm^{-3}$)
0	0	1/4	NA	Frozen methane (~10 K)	Clear	0.5
2×10^{16}	100	1/3	1/1	50% organic residue (~300 K)	Yellow	0.5
5×10^{16}	250	1/2	1/0.7	75% organic residue (~300 K)	Brown	0.5
1×10^{17}	500	1/1.5	1/0.5	90% carbonaceous (~300 K)	Black	0.75

*Ratio after heating to 300 K.

High-speed shutter video and computerized image processing indicate that the trajectories of the particles are not ballistic but reflect a continuous transfer of momentum from gas to dust and thus cause acceleration by gas-drag (Fig. 13b). The drag force, F_d, in the direction of the gas flow on a dust particle is given by the classical drag equation:

$$F_d = \pi s^2 \tfrac{1}{2} C_D \rho_g v^2 \quad (3)$$

where s is the particle radius, C_D is the drag coefficient, ρ_g is the gas density, and v is the velocity of the gas relative to the dust particles. The Earth's gravitational force on a dust particle, F_G, is:

$$F_G = 4/3\,\pi s^3 \rho_d g \quad (4)$$

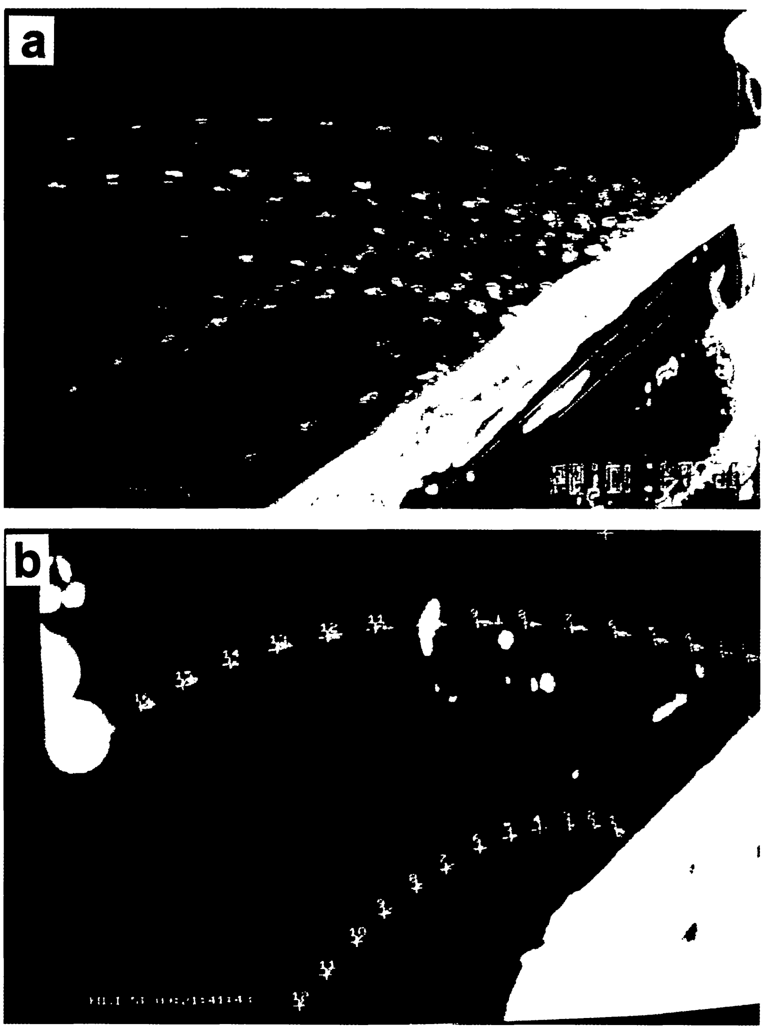

FIG. 13. Television images of surface activity during insolation in the KOSI apparatus. (a) A dust burst seen in false colors leaving the tilted surface of the sample. Some dust particles are emitted at high velocity and at steep angles relative to the surface, whereas others have curved shallow trajectories. (b) T.V. images showing the trajectories of two particles leaving the surface at different locations. The numbers indicate 0.02 s time intervals. Also shown are computed trajectories: the simple ballistic trajectories (green) stay close to the surface whereas the trajectories corrected for gas-drag (red) pass through the observed particle trajectories (Kochan and Koerver, 1991).

where ρ_d is its density of the particle and g is the acceleration due to gravity (9.81 m/s^2). The trajectories calculated by Grün *et al.* (1993) for emitted particles assuming gas-drag are shown in Fig. 14.

Thiel *et al.* (1991) found that the flux of ice-free particles decreased from ~100 to ~0.1 particles/45 μm interval/cm^2 as particle size increases from ~200 to ~500 μm. The angle of emission and velocity of the particles also depended on size. A central beam of low-velocity, large grains was surrounded by a background of high-velocity, small particles. Figure 15 shows histograms of ice particles of four mass ranges detected 89 and 128 cm from the sample as a function of time from the KOSI 9 experiment. A maximum flux of ~30 particles/15 min was reached at a range of ~89 cm. About half the particles were in the smallest size range (1–4.5 ng).

Reduction of Gas Emission Because of the Dust Layer–Ibadinov *et al.* (1991) derived quantitative empirical relationships between sublimation rate, mantle thickness, time, and depth using comet analogue experiments and the apparatus shown in Fig. 9a. They found that the mantle thickness, H, increased with time according to:

$$H = C\,t^{1/2} \quad (5)$$

in which C is a constant depending on energy fluence (C values of 2.3×10^{-5}, 1.45×10^{-5}, and 0.4×10^{-5}, corresponding to 1.3, 0.86, and 0.32 kW m^{-2}, respectively) and t is time (in seconds). For a sublimation rate for the water, I (in units of 10^{-4} g cm^{-2} s^{-1}), they found that:

$$I = 0.5\,C^2 \rho / H \quad (6)$$

where ρ is the density of the ice. Ibadinov *et al.* (1991) used these relationships to determine the mantle thickness and sublimation rate for Halley's comet. In the inner regions of the solar system, they found sublimation rates of 10^{-6} to 10^{-7} g cm^{-2} s^{-1} and mantle thicknesses of ~1 cm. It is unclear whether Ibadinov *et al.* corrected for the amount of Comet Halley's surface that was inactive, and this might imply that their estimated activity is lower than the comet's by an order of magnitude or so.

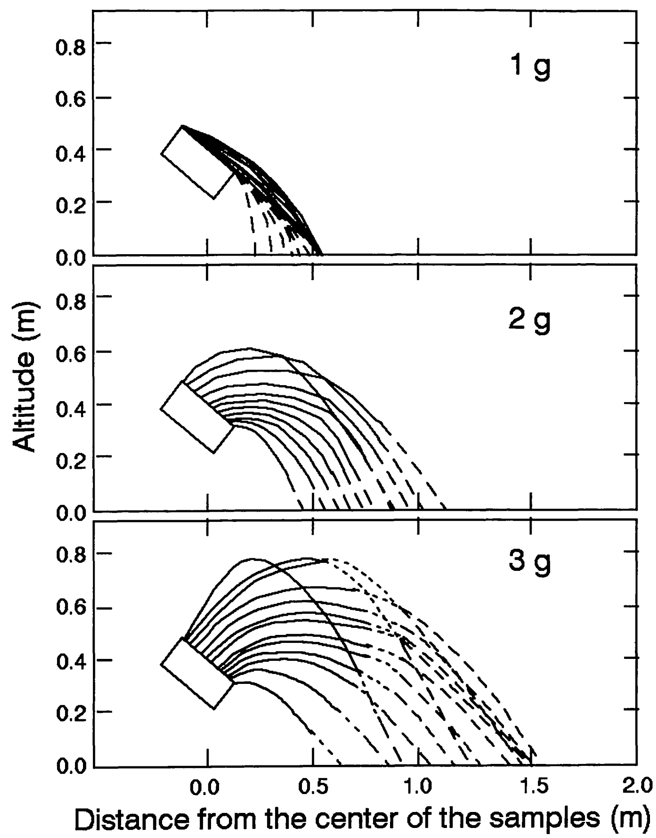

FIG. 14. Calculated trajectories for dust particles emitted at different positions along a center chord. Particle accelerations at 1, 2, and 3× acceleration due to Earth's gravity by gas drag at the surface have been assumed. The sample radius is 15 cm (Grün *et al.*, 1993).

Compositional Changes during Insolation

Dust-to-Ice Ratio–Mauersberger *et al.* (1991) examined 1200 ice particles (2 × 10^{-10} to 10^{-5} g) by measuring pressure changes caused by their evaporation upon landing on a heated plate 0.5 m from the surface of the KOSI samples. Brief signals were produced by pure ice particles whereas ice and dust particles produced longer pulses. The ratio of silicate to ice dust rose to ~200 during the first hour of the experiment and remained at this value for many hours. As mentioned above, silicate, CHON, and mixed silicate-CHON particles being ejected by comet P/Halley were detected by the *Giotto* spacecraft.

Thiel *et al.* (1991), using the particle collectors and piezo-impact detectors in the KOSI apparatus, found that the ratio of ice-free to ice-containing particles decreased from ~13 to 0.77 as particle size increases from ~200 to ~500 μm. This ratio could be higher for particles smaller than the 200 μm detection limit of the piezo detectors.

Dust-to-Gas Ratio–The KOSI-3 experiment produced a maximum gas flux density of 140 × 10^{16} molecules cm^{-2} s^{-1} and particle count rate of 60 s^{-1} (Kölzer *et al.*, 1995). For the KOSI-9 experiment, these values were typically 4 × 10^{17} molecules cm^{-2} s^{-1} and 30 particles/15 min period (Grün *et al.*, 1993). It is clear that dust-to-gas mass ratios observed during these experiments were many orders of magnitude below those observed for Halley's comet. This is an important discrepancy. One reason is that the atomic O/Si

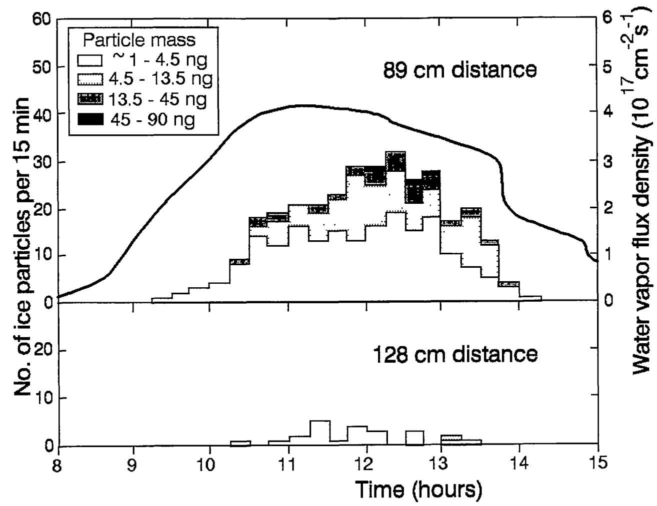

FIG. 15. Histograms showing impact rates for ice particles at 89 and 128 cm projected horizontal distance from the center of the sample's surface for the second irradiation period of the KOSI-9 experiment. The continuous curve shows the mean flux of water vapor at the surface. (After Grün *et al.*, 1993).

ratio for the comet analogues was ~14, compared to the solar or chondritic value of ~5.6. The DIDSY experiment on *Giotto* found a gas-to-dust mass ratio of 7:1–1:1, the range depending on the mass range integrated to determine the total mass of ejected particles (McDonnell *et al.*, 1987). In fact, because the largest mass detected was below that expected to be ejected, Grün and Jessberger (1990) suggest that these estimates should be increased by a factor of 3. Cosmic abundances suggest that the dust-to-gas mass ratio should be 1:1–2:1, assuming that all the dust was entrained by the gas.

Gas Composition–The H_2O/CO_2 molar ratio in the gas release of the KOSI experiments was usually found to be 6:1 to 3:1, compared with typical values of 14:1 for the ice in comet analogue. The higher abundance of CO_2 relative to H_2O in the gas, relative to the solid, results from the greater volatility of CO_2 than H_2O (Grün *et al.*, 1991c).

Once released into the coma, UV photolysis triggers a complex series of kinetically controlled reactions. Rössler *et al.* (1992a) made a detailed study of the UV photolysis products of the solids in the KOSI comet analogues using mass spectroscopy. Theoretical studies of the kinetic pathways have been made by several authors and recently reviewed by Jackson (1991) and Huebner *et al.* (1991). Polyoxymethylene has been reported by Huebner (1987) to be present in comets. This polymer breaks down to H_2CO and subsequently to CO. The kinetics leading to C_2, C_3, NH, SH, *etc.* have been studied in special detail.

Volatile Enrichment at Depth–Because of the greater volatility of CO_2 compared to H_2O, a CO_2/H_2O profile develops with depth in the sample (Hesselbarth *et al.*, 1991). Thus the surface layers are CO_2-depleted and the CO_2/H_2O ratio increases abruptly below the CO_2 sublimation layer, due to recondensation, and then decreases slowly with depth (Fig. 16).

Hesselbarth *et al.* (1991) found that the concentration of CO_2 in the surface layers of comets follows the equation:

$$\partial c/\partial x = (1-\gamma)\, c \exp\left[-(x - x_{sub})/s\right] \Big/ \int \exp\left[-(x - x_{sub})/s\right] dx \quad (7)$$

where γ is the fraction of CO_2 leaving the surface, s is a "penetration depth" (a theoretical construct to make diffusion length dimension-

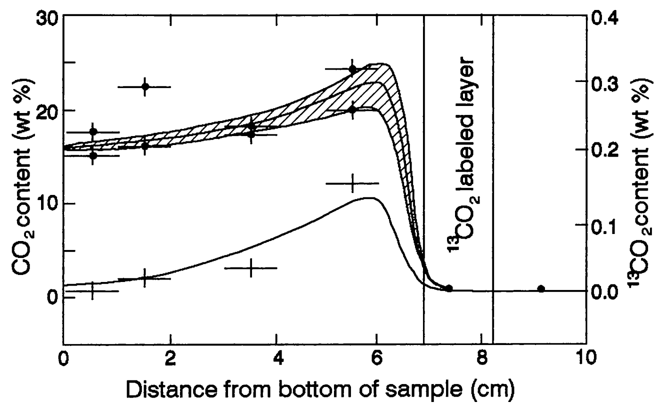

FIG. 16. The $^{12}CO_2$ concentration (left-hand axis, filled symbols) and $^{13}CO_2$ concentration (right-hand axis, error bars without data points) as function of depth in the KOSI 4 sample after irradiation. The $^{12}CO_2$ was initially uniformly distributed throughout the sample at 15 wt%, whereas the $^{13}CO_2$ was originally located only at depths of 6.9 to 8.2 cm. The curves are given by Eq. (7) in the text, where c = 0.4 and s = 2.5 cm. The shaded area corresponds to a range in c of 0.32 to 0.54. Sublimation of CO_2 at ~7.5 cm caused its loss by evaporation outwards and recondensation at greater depth (Hesselbarth *et al.*, 1991).

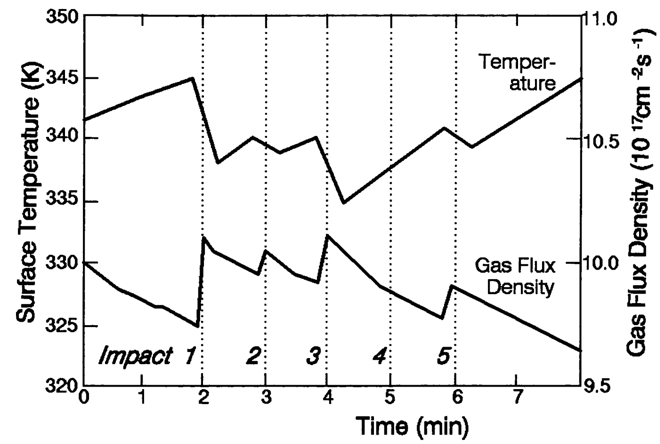

FIG. 17. Local surface temperature and global gas flux during the KOSI 10 impact events. The impact of different amounts of "Terraperl" particles in the size ranges given cause pulses in the gas flux density of different peak heights. The uncertainties in the maxima and minima for the temperatures are ±10 to ±15 s and for the gas emissions are ±2 s (Thiel *et al.*, 1995).

less), c is the CO_2 concentration at depth x, and x_{sub} is the experimentally observed depth of the sublimation front. The integration is performed between the sublimation front at x_2 and sample depth. The best-fit curve for the data was obtained when γ was between 0.32 and 0.54 and s was 2.5 cm.

Isotope Fractionations–Isotopic fractionation during the KOSI experiments was measured by Klinger *et al.* (1989) and Rössler *et al.* (1992b). They found ΔD values for the interior and mantle of –47.7 and –35.7‰ (relative to SMOW), respectively; and for $\delta^{18}O$, they found values of –6.40 and –4.27‰. (Where δ is the difference in the D/H, $^{17}O/^{16}O$, or $^{18}O/^{16}O$ ratios in parts per thousand between a sample and standard, standard mean ocean water (SMOW). For the primitive Orguiel CI chondrite, δD and $\delta^{18}O$ values are –50.5 and –7.05‰, respectively). Thus, as expected, mass fractionation causes the surface of the KOSI samples to be enriched in the heavy isotopes whereas the interior is essentially unchanged.

Impact-induced Effects during Insolation

Stern (1988) has argued that impacts of centimeter-sized particles onto kilometer-sized comet nuclei could have been significant over the lifetime of a comet in the Oort Cloud, and this impact rate might be expected to be higher in the inner solar system. The effects of micrometeorite bombardment of a comet nucleus surface were explored by Thiel *et al.* (1995) who impacted "Terraperl" particles of various sizes at relatively low velocities onto the surface of the KOSI 10 sample. "Terraperl" is a pumice-like silicate glass with a density of 0.09 g cm^{-3}, which is assumed to approximate the grains ejected from the surface. The impacts disturbed the dust mantle and caused 1-7 K drop in temperature, depending on impactor size, and increased the gas flux and thereby the gas drag on escaping particles (Fig. 17). Particle accelerations of <10 to 17 m s^{-2} were observed, depending on particle size. All these processes are expected to occur on comets under the appropriate circumstances.

Thermal Behavior during Insolation

Thermal Conductivity–Thermal conductivity data are required for thermal modeling of the comet nucleus, but equally important is a quantitative understanding of the physical processes that occur in the surface layer of the comet nucleus. The theoretical models can be compared with the results of the large-scale simulations. Values for the thermal conductivity of snow, snow–ice, and snow–dust mixtures with porosities similar to those of the KOSI samples were measured by Spohn *et al.* (1989a,b). They used a 70 mm diameter, 125 mm long cylindrical sample heated at one end and cooled at the other, with thermocouples located throughout. Thermal conductivity values ranged from 0.15 to 0.65 W m^{-1} K^{-1} with little or no dependence on temperature over the range 80 to 170 K or on mineral grain content. In contrast, regions containing crystalline ice had a thermal conductivity of 3.5 to 8 W m^{-1} K^{-1}, about a factor of 10 larger than poorly crystalline regions of the comet analogues. Benkhoff and Spohn (1991) reported matrix thermal diffusivity values of 2–13 × 10^{-8} m^{2}s^{-1} at 125 K. (Thermal diffusivity, $\kappa = K/(\rho\ C)$, where K is thermal conductivity, C is the specific heat, and ρ is bulk density. Specific heats were ~1 MJ m^{-3} K^{-1}, except for the KOSI 5 sample for which the value was 0.4 MJ m^{-3} K^{-1}).

Kossacki *et al.* (1994) have discussed the influence of grain sintering on the thermal conductivity of porous ice. The sintering of ice grains, which leads to a continuous growth of the grain to grain contact area (Hertz factor), was incorporated into a thermal evolution model. The sintering process was found to lead to significant changes of the matrix conductivity on timescales of hours to days. In simulation experiments with paraffins with a water–mineral mixture, Kömle *et al.* (1996) found that a cohesive residuum was formed that had a thermal conductivity an order of magnitude higher than the typical unconsolidated dust mantle.

Temperature Profiles–Theoretical studies of thermal profiles in comet materials by Mekler *et al.* (1990), Spohn and Benkhoff (1990), and Espinasse *et al.* (1991) have been conveniently summarized by Rickman (1992). Typical temperature profiles through the KOSI samples are shown in Fig. 18. There is a steep temperature gradient through the dust mantle (when present—see KOSI 5 data), and a shallower gradient below the mantle with discontinuities at ~210 K due to the sublimation front of H_2O and 125 K due to the sublimation front of CO_2. Most remarkable are the convex profiles sometimes shown. These cannot be explained by conduction alone and require redistribution of heat by vapor transport (Hsiung and Rössler, 1989; Grün *et al.*, 1991b; Rössler *et al.*, 1990, 1992c; Benkhoff *et al.*, 1995).

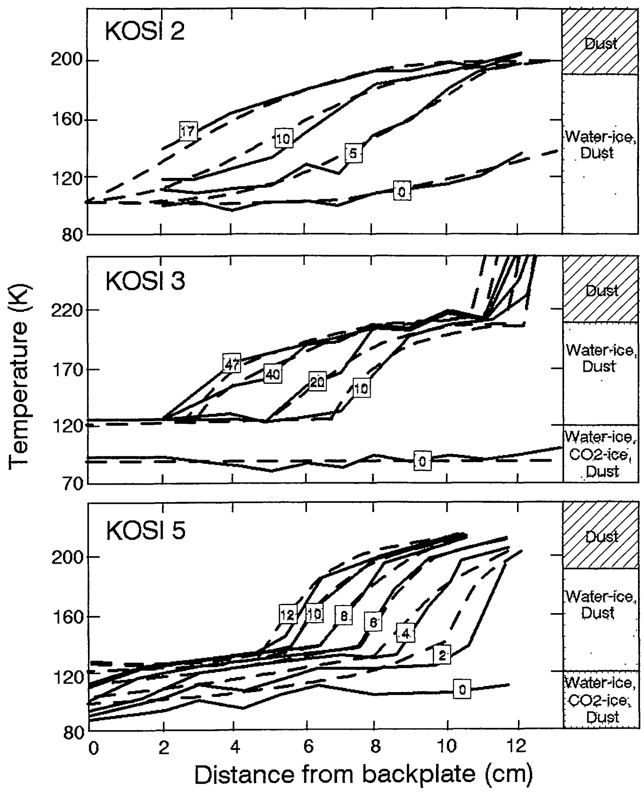

FIG. 18. Temperature profiles in three KOSI experiments. In all cases, the temperatures increase from the cooled backplate to the illuminated surface, and the profiles became steeper with time. The KOSI 3 and 5 profiles show discontinuities in the rate of increase due to a water-ice sublimation front at 210 K and a CO_2-ice sublimation front at 125 K. The CO_2 front moves faster because of the higher volatility of and smaller amount of CO_2. The broken lines refer to theoretical calculations. The numbers refer to elapsed time in hours. (Benkhoff and Spohn, 1991).

The thermal diffusion equations for modeling heat transfer through solids are:

$$C\rho\ \partial T/\partial t + C_g f_g\ \nabla T = \mathrm{div}(K\ \nabla T) - HQ_g \quad (8)$$

$$\partial \rho_g/\partial t = -\mathrm{div}\, f_g + Q_g \quad (9)$$

where C, ρ, K are the heat capacity, density, and thermal conductivity of the solid phase, respectively; C_g, f_g, and Q_g are the heat capacity, mass flux, and mass release rate of the vapor, respectively; and H is the latent heat of sublimation. The production rate of vapor can be described by the kinetic theory of sublimation:

$$Q_g = S[p_v(T) - \mathrm{p}]\ \surd[m/(2\,\pi\, kT] \quad (10)$$

In which S is the surface/volume ratio of the porous matrix, $p_v(T)$ is the vapor pressure, and p is the local pressure. Surface boundary conditions (*i.e.*, heat balance at the surface) are imposed by Eq. (11) and assuming $p_s = p_v(T)$.

$$E_{in}(1 - a_b) = \epsilon\ \sigma\ T_S^4 + K\ dT/dR|_S + H(T_s)Z(T_s) \quad (11)$$

where E_{in} is the heat flux falling on the surface, a_b is the Bond albedo, ϵ is the IR emissivity, σ is the Stefan-Boltzmann constant, K is thermal conductivity, T_S is the surface temperature, R is the coordinate normal to the surface, $H(T_s)$ is the latent heat of sublimation of the ice, and $Z(T_s)$ is the gas flux passing through the surface. The first term on the right represents radiation loss from the surface. It is important that the latent heat of vaporization is consistent with the vapor pressure. This requirement (the Clausius-Clapyron equation) has not always been obeyed in model calculations.

Huebner and Boice (1992) have discussed three-dimensional time-dependent theoretical modelling of surface layers: energy balance at the surface, thermal properties of ice and dust–ice mixtures, and recondensation at the surface.

OBSERVATIONS MADE FOLLOWING INSOLATION

The Outer Layers of the Nucleus

Surface Topography–The surface topography of the KOSI samples was caused through dust removal by gas drag and, on inclined surfaces, by avalanches and slippage. Valleys and ridges were formed on the surface. Grün *et al.* (1993) described a situation in which there was surface movement during the KOSI 9 experiment (200–1900 W/m^2, 10 wt% olivine in ice). During the first experimental period of insolation, gas and particle flow decreased and temperature increased after a mantle had formed. When gas flow reached 10^{21} H_2O molecules m^{-2}s^{-1} during the second period, an avalanche occurred on the surface that damaged the mantle and exposed fresh ice and enhanced gas and dust production. Many of the dust grains were fluffy aggregates. No damage to the mantle occurred during the third period, and gas and dust flow was not enhanced.

The high sublimation rate at the beginning of the experiment resulted in the rapid formation of a mantle that became an obstacle to further heat and gas flow from the nucleus (Grün *et al.*, 1991c). Grün *et al.* (1993) found that the dust mantle caused the redistribution of heat throughout the sample by gas transport and that a build-up of pressure could cause disruption of the mantle and erratic and systematic variations in comet activity (Grün *et al.*, 1993). This occurred despite the mantle being fairly porous. Figure 19 shows an emission of dust (Fig. 19a) caused by an avalanche on the sample surface (Fig. 19b) and the exposure of a fresh ice- and mineral–matrix that resulted in a cold spot (Fig. 19c; Lorenz *et al.*, 1995).

Stratigraphy of the Outer Layers–Figure 20 shows sketches of sections through the KOSI 3-7 samples after irradiation. The KOSI 4 sample experienced relatively low fluence whereas the KOSI 6 sample was mineral rich. These factors resulted in low levels of activity and little emission of gas and dust. In contrast, the methanol in the KOSI 5 sample and the low mineral content of the KOSI 7 sample seems to have resulted in high activity and major changes in stratigraphy, presumably because of the volatility of methanol and absence of moderating effects of the dust. The KOSI 9 results are summarized schematically in Fig. 21.

The thermal wave into the sample results in a complex stratigraphy in the icy layers under the dust mantle. Rickman's (1991) summary of the processes expected to occur in a real comet is described schematically in Fig. 22. The simulation experiments did not include amorphous ice, and this must be considered in comparing this figure to the KOSI results. Evaporation of water and other volatiles leads to the production of the refractory dust mantle on the surface, and the heat wave penetrating the nucleus results in a crystallization front and an evaporation front. The loss of volatiles causes erosion of the surface, whereas crystallization results in the liberation of heat. Evaporation results in transport of gases, especially the more volatile CO_2. The CO_2 redistributes heat as it diffuses through the pore-space in the comet. There is an outward flow of CO_2 to the surface and an inward flow to somewhat deeper, cooler regions where it recondenses.

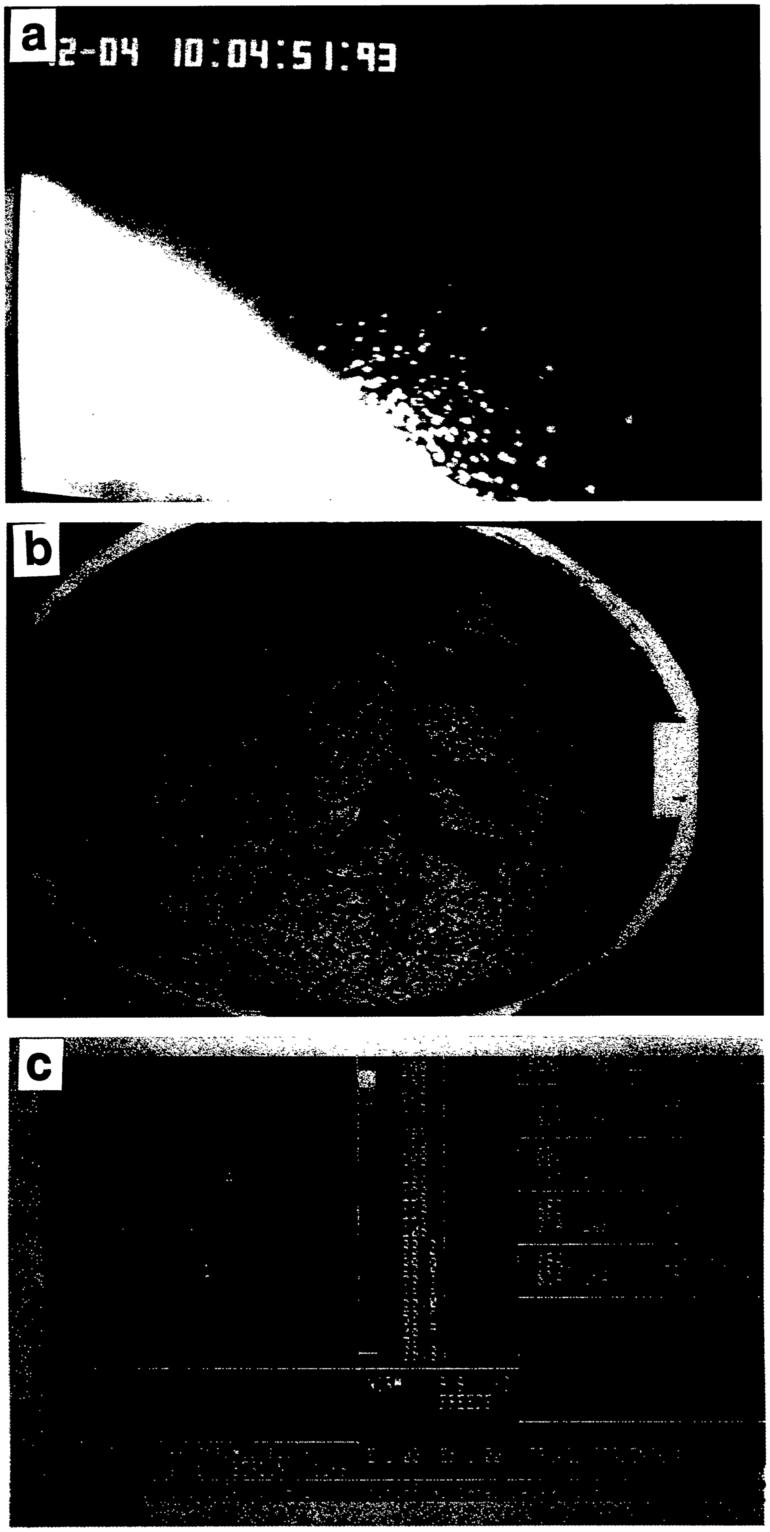

FIG. 19. (a) Dust burst leaving the surface of a KOSI sample as a result of an avalanche. (b) Surface of one of the KOSI comet analogue samples during insolation. The lower two arrows are indicating the extent of an avalanche that has occurred on the surface of the sample. (c) During the avalanche and dust burst shown in Fig. 19a,b, the IR camera detected a fresh cold spot on the surface. (Courtesy of E. Lorenz, DLR).

Most of these expectations are borne out by the KOSI experiments. There are dust-rich surface regions, crystallization fronts, H_2O-rich regions with large crystals, an inner crust and regions of solidification, layers of ethanol or methanol crystals, and CO_2 and H_2O crystals. Comet analogues of water, methanol, and CO_2 produced icy layers of these species at different depths; and because temperature decreases with increasing depth, the formation of the internal layers follows the crystallization temperature of the different components. Thus real comets that contain a large variety of volatile components probably contain an onion-skin structure of these layers. This effect was named "thermochromatography" by Hsiung and Rössler (1989).

Nature of the Comet Analogue Material

Strength Parameters–Penetration strength is important to comet nucleus *in situ* measurements and sample return missions because it will determine landing techniques and the design of drilling and anchoring equipment. Kochan *et al.* (1989c) have reported penetration measurements—the force required to push a 0.5 mm diameter Teflon rod with a hemispherical tip into the samples at 0.2 mm/s—on KOSI comet analogues after irradiation (Fig. 23). Figure 23 shows the KOSI 5 sample in the glove-box during the hardness test with the penetrometer.

All KOSI experiments produced a hard surface layer where volatile compounds volatilized or diffused inwards crystallized. However, strengths, thicknesses, and the depths at which the layers formed varied from sample to sample. Where recrystallization of water vapor was extensive, stress values of 0.2 to 5 MPa were observed; but in areas where it was less extensive, values were only 0.05 to 2 MPa. Below 200 K, crystallized ice in these experiments has strengths of ~5 MPa. Thus, as might be expected, the penetration strength of the material depends very strongly on porosity, with poorly crystallized ice having values one-tenth to one-hundredth those of crystallized ice, or less.

The compressive strength of the comet analogues was measured as a function of temperature, density, and composition by Jessberger and Kotthaus (1989; Fig. 24). Standard triaxial and uniaxial cells were used at 123, 233, and 253 K with a 10 MPa force and 1 mm/min displacement. Compressive strength decreases from 8 to 1 MPa with increasing temperature, decreasing density (from 0.8 to 0.5 g cm^{-3}), and increasing proportion of dust and tuff fragments (0 to 50%).

Density and Porosity–Comet analogue starting materials are usually of low density (0.4 to 0.60 g cm^{-3}), high porosity (29 to 50%), and low albedo (0.07 to 0.20) (Table 3). Porosity and water content seem to correlate and are inversely proportional to density, but CO_2 and dust do not appear to play any systematic role in determining albedo, porosity, and density (Fig. 25). Thiel *et al.* (1995) showed that the porosity and density of the sublimation residues depends on particle size, and they proposed exponential relationships with decreasing density and increasing porosity as particle size increases (Fig. 26) and densities are comparable to those of Halley's comet (Table 8). However, albedos of the analogues are some-

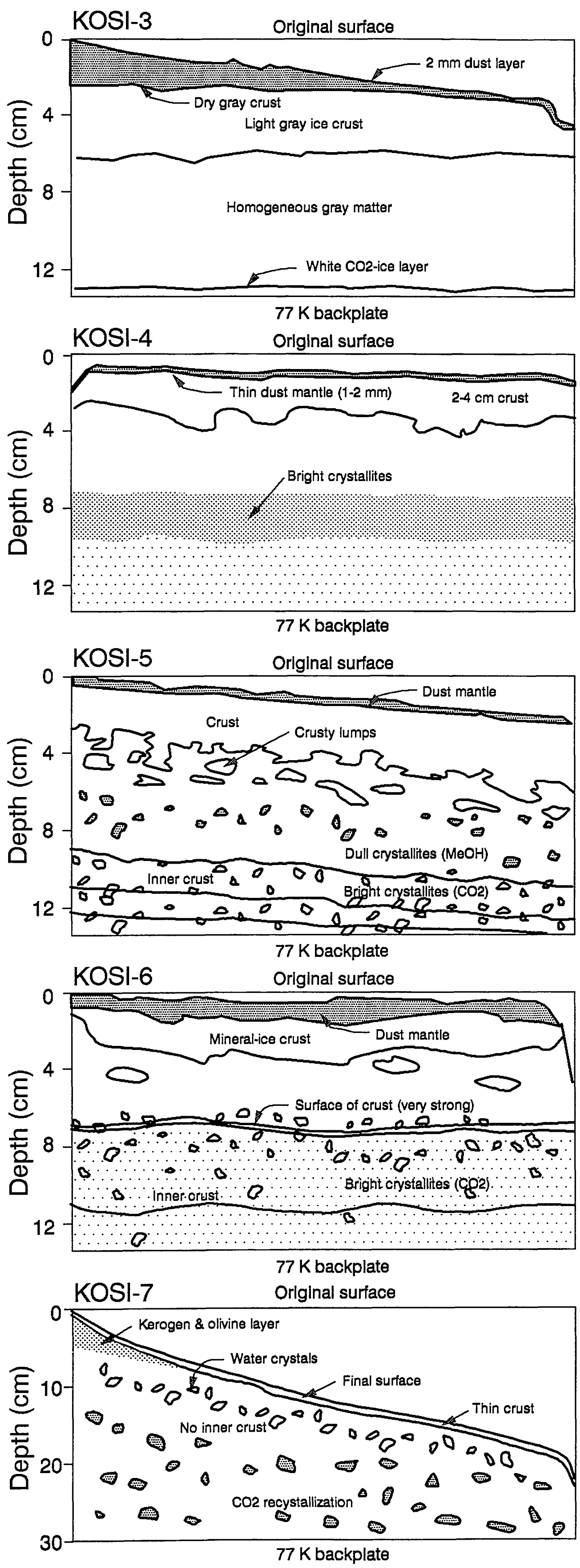

what higher and the processes in the laboratory are totally different to those in comet nuclei.

Spectral Reflectivity and Albedo–Oehler and Neukum (1991) have reported the spectral reflectivity data for the visible and near IR region (0.36–2.5 μm) for the KOSI 3,4,6 experiments, and Grün *et al.* (1991c) mention data for the KOSI 3 experiment. The measured albedo values were 10 to 20% with errors of <10%. Some experiments resulted in small decreases in albedo, but others showed a surprising increase attributed to frost that formed after the experiment. The 1–5 mm dust mantle produced on these samples caused a decrease in the H_2O and CO_2 absorption features at 1.5 and 2.0 μm, but again a water–ice absorption band that appeared after the irradiation was thought to be due to frost.

Petrographic Studies–Stöffler *et al.* (1991) and Stöffler and Düren (1992) have developed procedures for preparing thin sections of comet analogue material adopting methods used for snow research. They impregnate the samples with diethyl phthalate at 268 K and then freeze, cut, and section them at 253 K, a special sledge microtome being used to make the thin sections. The sections can then be examined under optical microscopes in a cold room at 258 K (Fig. 27).

Pure water–snow crystals present in the KOSI analogue material showed increased grain size as the samples increased in porosity. Snow–ice and dust mixtures had a loosely consolidated dust on the surface after exposure in the KOSI apparatus due to sublimation of ices from the surface. Below the dust layer, a "hard" layer was formed by recondensation and recrystallization of H_2O and CO_2. Sometimes the surface dust contained pure clear ice crystals of ~200 μm grain size.

Stöffler *et al.* (1991) and Stöffler and Düren (1992) have proposed that the complex petrography of ice and dust assemblages may be present in returned comet samples. They list polycrystalline ices and clathrates, polycrystalline inorganic mineral aggregates (rocks), composite polycrystalline polyphase aggregates, fluffy aggregates of frozen volatiles, fluffy dust aggregates, and fluffy aggregates of ices and refractory dust.

Comet particles are often compared with interplanetary dust particles (Brownlee, 1985; Sandford and Walker, 1985; McKinnon and Rietmeijer, 1987; Bradley, 1988) and CI chondrites (Kerridge and Matthews, 1988), although a detailed study has yet to be made. Studies of terrestrial ice cores and alterations suffered near their exposed surfaces might also provide further insights.

TABLE 8. Density and albedo estimates for the nucleus of Halley's comet.

Density (g cm^{-3})	
0.5	Rickman and Huebner (1990)
0.3–0.6	Greenberg and Hage (1990)
0.5	Hughes (1981)
0.7	Wallis and MacPherson (1981)
0.28 (0.2–0.7)	Rickman (1986, 1989)
Albedo*	
$0.04^{+0.02}_{-0.01}$	Sagdeev *et al.* (1986)
0.02–0.05	Divine *et al.* (1986)
0.032 (1.25 μm)	Tokunaga *et al.* (1986)
0.045 (1.65 μm)	Tokunaga *et al.* (1986)

*At visible wavelengths unless otherwise stated.

FIG. 20. (left) Sketches of the textures through the surfaces of five of the KOSI comet nucleus analogues after irradiation in the large simulator at DLR. The samples are mounted at an angle of 40° with their right side as drawn here, higher than the left side. Hence some slippage to the left. (From Hsiung and Rössler, 1989; Rössler *et al.*, 1990, 1992c).

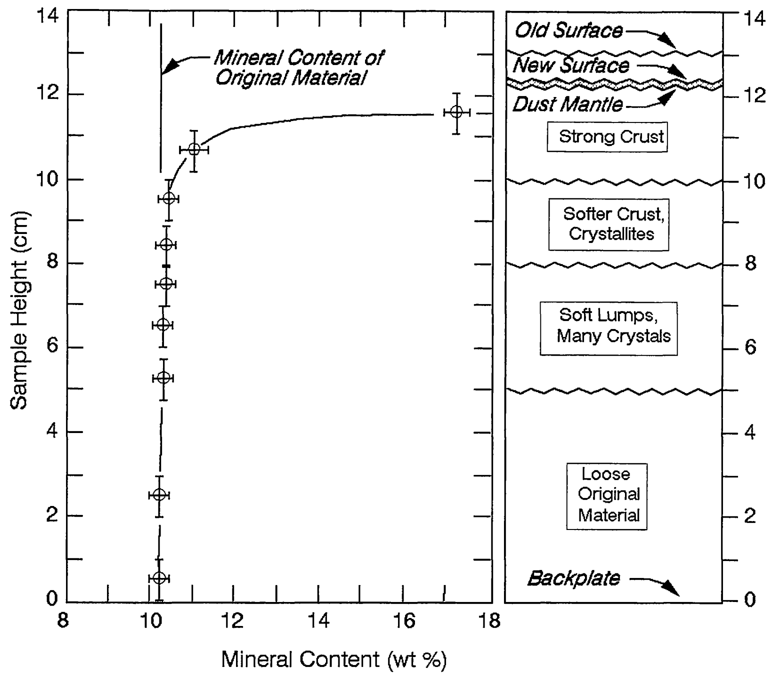

FIG. 21. Mineral content as a function of depth and the macroscopic stratigraphy of the KOSI 9 sample (10% dust, 90% water ice) after irradiation (Grün *et al.*, 1993).

The Silicate Dust

Morphology of the Silicates–The silicate residues produced by Saunders *et al.* (1986), using the apparatus in Fig. 8b, were botryoidal aggregates of grains (Fig. 28a) and highly porous filamentary structures (Fig. 28b). The latter are of special interest because many scientists expect comet silicates to resemble them. The filamentary residues had high tensile strength, high porosity, low density, and were electrically conductive. Thiel *et al.* (1995) found that similar sublimation experiments with montmorillonite also produced aggregates with high electrical conductivity. Storrs *et al.* (1988) were able to explain most of the properties of these filaments by assuming that they are chains of grains bound by electrostatic forces (Fig. 29). They suggest that impurities are swept from clay minerals in the ice and that the minerals are then removed by entrainment in the escaping volatiles. The cleaned, dried, and electrostatically charged clay minerals then form chains that are electrically conducting by virtue of the interlayer water. The filamentary structures described by Storrs *et al.* (1988) and Saunders *et al.* (1986) were only produced by clay minerals, and not hydrated silicates.

Donn (1991) has reviewed some of the expectations for the morphology of the precursor materials that agglomerated into comets. Looking at the structure of a number of materials made by condensation or similar processes (and computer predictions), he argues that material accumulating at low temperature in the interstellar environment would be low density, filamentary clusters (Fig. 30a–d). The filamentary residue structures of Saunders *et al.* (1986) show first order similarity to some of these expectations. Thus most scientists have argued that the silicates in comets will have a fluffy, low-density structure. The structures are also reminiscent of dust particles collected in the stratosphere (Fig. 30e; Brownlee, 1985), although the degree of alteration and selectivity suffered in interplanetary space (during insolation) and during atmospheric passage must be significant.

Differences between Phyllo- and Nesosilicates–In the first 6 of the 11 KOSI experiments performed in the big chamber, a mixture of 90 wt% olivine (a framework, or nesosilicate) and 10 wt% montmorillonite (a lattice-layer, or phyllosilicate) was used in the dust sample preparation. For KOSI-1, 99 wt% kaolinite was used for dust. The emitted olivine particles during KOSI 9 had sizes of just over 100 μm and were aggregates of 0.2 and 3 μm olivine grains. It seems that these larger agglomerates were formed during the injection of the aqueous suspension into the liquid nitrogen (Fig. 8c). This clearly can be seen in Fig. 31a where a solidification front was running through the droplet producing a structure resembling dendritic branching. The sample was 10 wt% montmorillonite and 90 wt% water. Thiel *et al.* (1995) suggested that the montmorillonite platelets acquired their orientation during freezing of the solidification front. By contrast, Fig. 31b shows the structure of a particle emitted from a sample with 90 wt% water ice and 10 wt% olivine. In the case of a mineral admixture of merely olivine, the texture of the collected dust particle is highly irregular with low internal cohesion. The physical nature of the dust particles was thus predetermined by composition and sample preparation method.

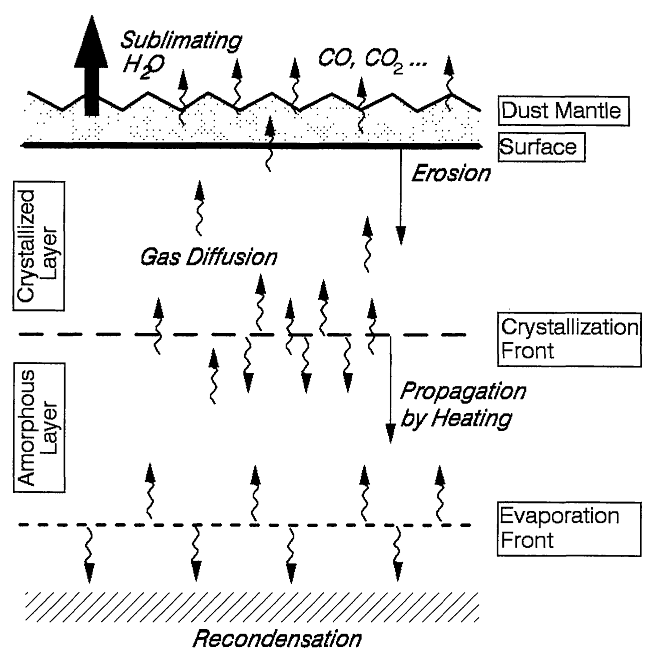

FIG. 22. Processes thought to be occurring near the surface of comet nucleus (Rickman, 1991). Sublimation of water at the surface results in erosion of the surface and the accumulation of a dust layer. The external heating crystallizes the ice that is assumed to have originally been amorphous, a process that may aid in the release of trapped gases. Evaporation occurs along a front at 210 K for water (and 125 K for CO_2) and the released gases can move outward, to ultimately escape into space, or inward, to recondense at lower temperatures. Thus heat is moved throughout the comet surface layers by both conduction and mass transport by gas diffusion as well as by vaporization and recondensation.

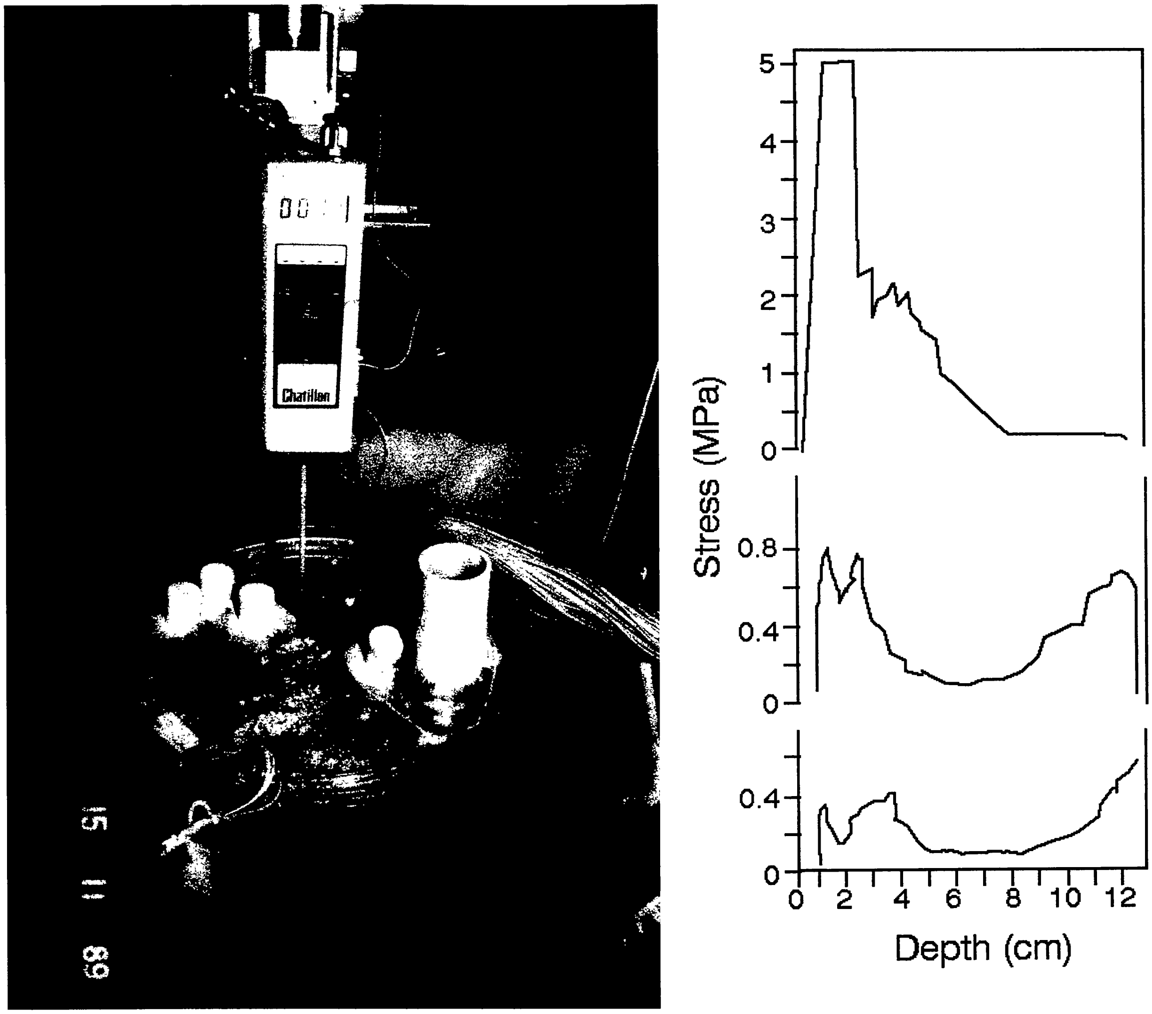

FIG. 23. Apparatus for determining the penetration strength of comet analogues (left) and examples of profiles from two samples (right). Upper profile, KOSI 4; middle profile, KOSI 3, 2.5 cm from the sub-illumination point; lower profile, KOSI 3, 6.0 cm from the sub-illumination point. The profiles seem independent of distance from the center of illumination. Although the profiles vary from experiment to experiment, the devolatilized surface layer always has higher strength than the interior (Kochan *et al.* 1989c).

ROLE AND LIMITATIONS OF LABORATORY SIMULATION EXPERIMENTS AND FUTURE DIRECTIONS

Comet simulation experiments can be used to address some of the engineering questions associated with comet nucleus missions, such as whether an experiment destined for a spacecraft has been adequately designed, whether it will pose and address the right questions, and whether the equipment will survive conditions likely to be encountered. The simulations also help with the interpretation of spacecraft data and can even help identify problems that are encountered during a mission and guide the design of procedures to overcome them. For example, Lafontaine *et al.* (1992) and Eiden and Coste (1992) discuss the need for immediate anchoring of the spacecraft and Oehler *et al.* (1992) used IR spectroscopy calibration data from comet simulations to determine surface temperatures of comets. Kömle *et al.* (1997) discussed the possibility of using the anchor to determine the mechanical properties of the surface. The drill bit designs, and acoustic sounding techniques used to derive internal structure, were also dependent on the comet simulation experiments (Kochan and Junglus, 1993). Simulation experiments could also provide some guidance for the topography that might

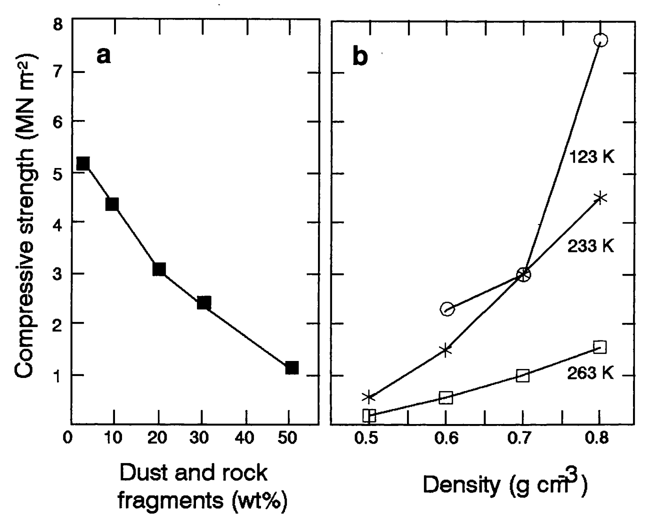

FIG. 24. Compressive strength of comet analogue materials as a function of (a) proportion of dust and (b) temperature and density (composition: H_2O, 75 wt%; olivine, 17 wt%; montmorillonite, 4 wt%; kaolinite, 4 wt%) (Jessberger and Kotthaus, 1989).

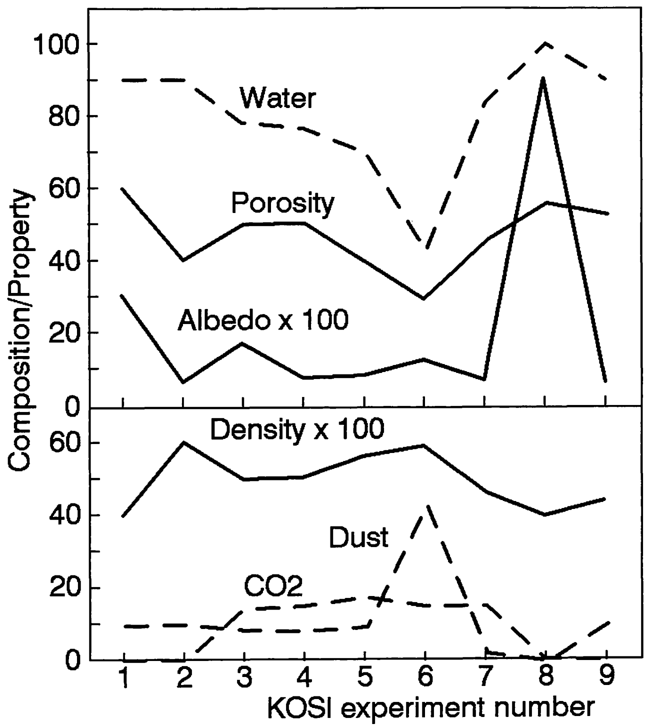

FIG. 25. The composition (water, CO_2, and dust content) and properties (albedo, density, and porosity) of the comet analogue materials for the KOSI experiments. Porosity and albedo seem to correlate with water content (notwithstanding the high albedo of the KOSI 8 sample) and are thus inversely proportional to density. The CO_2 and dust content do not appear to play any systematic role in determining albedo, porosity, and density.

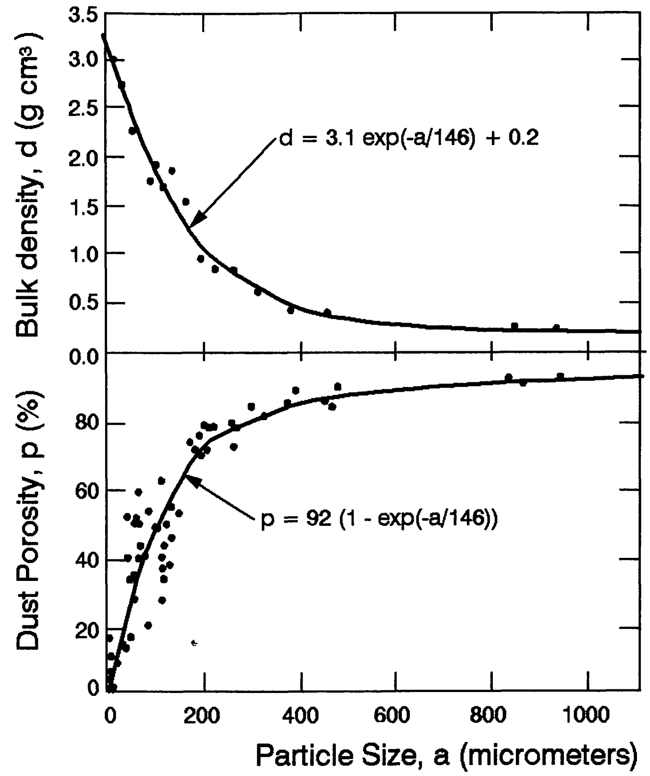

FIG. 26. Dust particle density and porosity as a function of particle size for comet analogue material made by pouring suspensions of dust in water into liquid nitrogen. The data are from the KOSI 9 experiment, but very similar data were obtained for the KOSI 5 experiment (Thiel *et al.*, 1995).

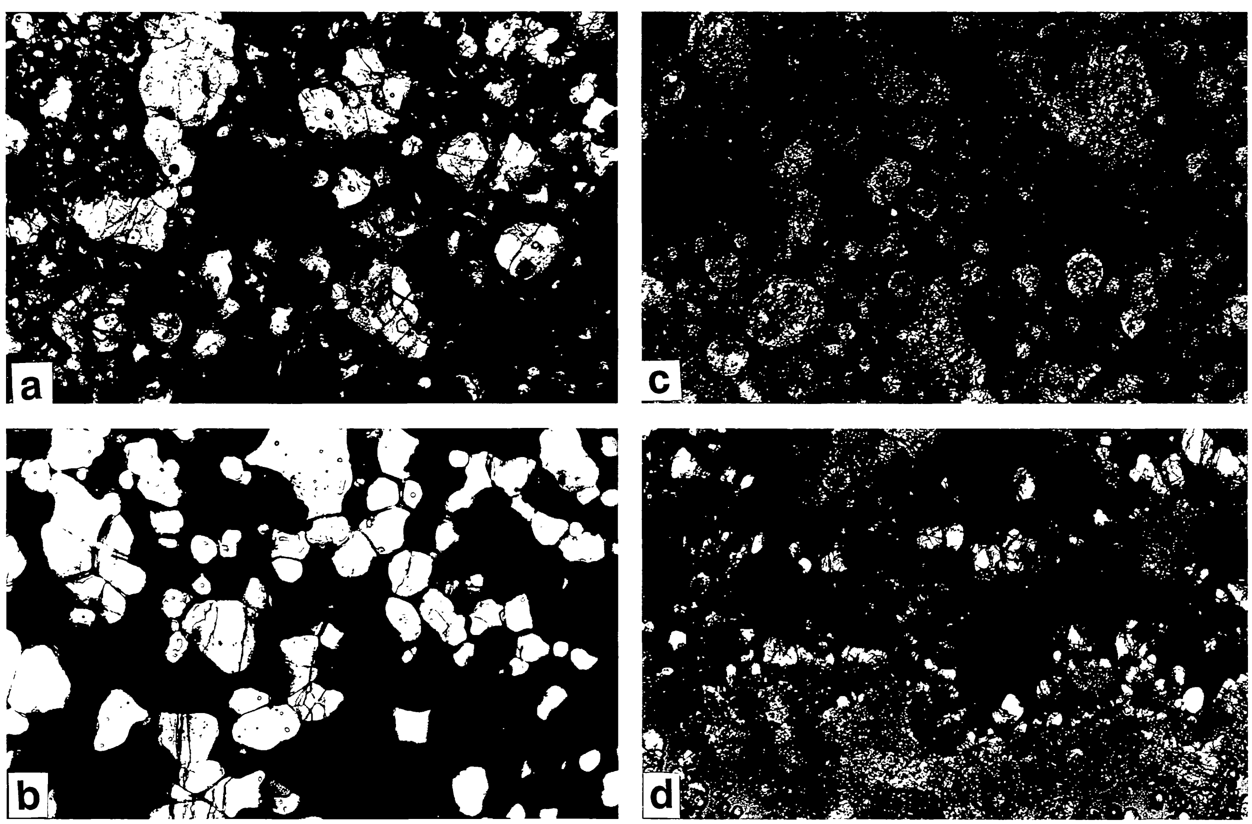

FIG. 27. Photomicrographs of pure water–snow comet analogue materials (a) before and (b) after irradiation. Pore space = dark. Ice crystals = white. Photomicrographs of water–snow and dust mixtures (c) before and (d) after irradiation. (Transmited polarized light: pore space = grey, ice crystals = mottled-white. 2.8 mm width of field. Stöffler and Düren, 1992).

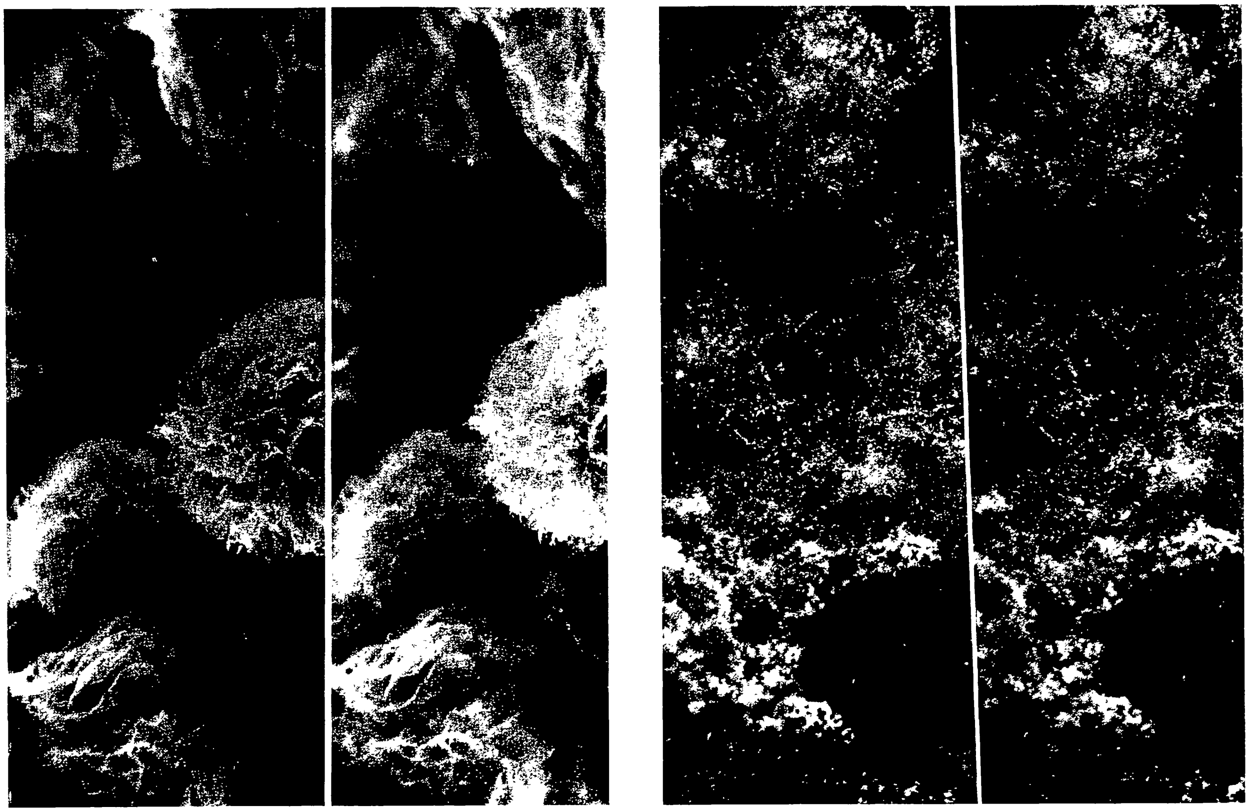

FIG. 28. Stereo images of sublimation residues produced by spraying a water-clay slurry into liquid nitrogen (see Fig. 8b). Left, botryoidal forms. Right, filamentary forms. Three-dimensional images can be seen by crossing one's eyes until the two small crosses are superimposed. Horizontal field of view is 125 μm. (From Saunders *et al.*, 1986).

make a landing possible. The KOSI experiments also stimulated the developments of heat and gas diffusion models for comet nuclei (*e.g.*, Prialnik, 1992; Kührt and Keller, 1994; Benkhoff and Boice, 1996; Coradini *et al.*, 1997a,b).

The major impetus for laboratory simulation experiments is to understand the physical and chemical processes likely to be occurring in or on a comet. Klinger *et al.* (1989) and Keller and Markiewicz (1991) present different perspectives on this topic. Klinger *et al.* (1989) point to a number of early results of the comet simulation experiments that have caused or should cause a revision to current ideas about comet processes. First, they point out that vapor phase transport of heat is important in determining the history of the comet nucleus. Secondly, they argue that more realistic estimates of thermal conductivity of comet solids may now be available. Third, they suggest that the dust mantle that forms on the surface of the nucleus does not prevent heat from penetrating the nucleus; to the contrary, the dust mantle may cause higher internal temperatures and pressures than would otherwise apply. These arguments are heuristic and based on limited model calculations. In view of the uncertainties in such models (see Huebner *et al.*, 1998), these arguments must be viewed with caution.

Keller and Markiewicz (1991) stress the difficulties of simulating comet processes. They argue that because the starting material used in the large-scale simulations is not produced by condensation, the large refractory grains might not be fluffy enough to be emitted from the nucleus by gas-drag. Rössler *et al.* (1990) tried to produce large comet analogues by the condensation of water vapor mixtures onto a liquid nitrogen cooled, rotating cylinder. The grain aggregates produced proved to be fluffy, but the sample could not be readily removed and the method was prohibitively slow. Another possible approach would be to inject a mixture of pulverized dust, water-vapor, and organic compounds into a liquid nitrogen cooled chamber in a way that the vapor can condense onto the dust grains.

Keller and Markiewicz (1991) also point out that the gravitational fields in the laboratory are three orders of magnitude stronger than on a comet. The influence of the Earth's gravitational field has also been discussed in the context of the emission of ice and dust particles. However, particles in comet analogues are not loosely deposited on the surface of the sample. High-resolution optics show them to be bonded to the ice–mineral matrix. Before they are free and can interact with the gases leaving the samples, the bonds have to be eroded by sublimation of the ice attaching them to the surface. Calculations based on these observations have shown that the binding force is orders of magnitude stronger than the force resulting from the Earth's gravitational field meaning that the laboratory simulations are reproducing the cosmic conditions (Ratke and Kochan, 1989).

Thirdly, comet models are 10^{-5} to 10^{-7} times those of comet nuclei in size, and temperature gradients inside the analogues are ~100 times greater than in comets. Finally, Keller and Markirewicz (1991) argue that the timescales for laboratory experiments are necessarily quite different from those of the cosmos. Thus gas flow from sublimating ice, interactions of gas and dust, and heat transport properties cannot be accurately related. These are obviously reasonable criticisms, and clearly the comet simulations are only applicable to conditions in the vicinity of the nucleus and then only on the centimeter to meter scale. However, probably the major uncertainty

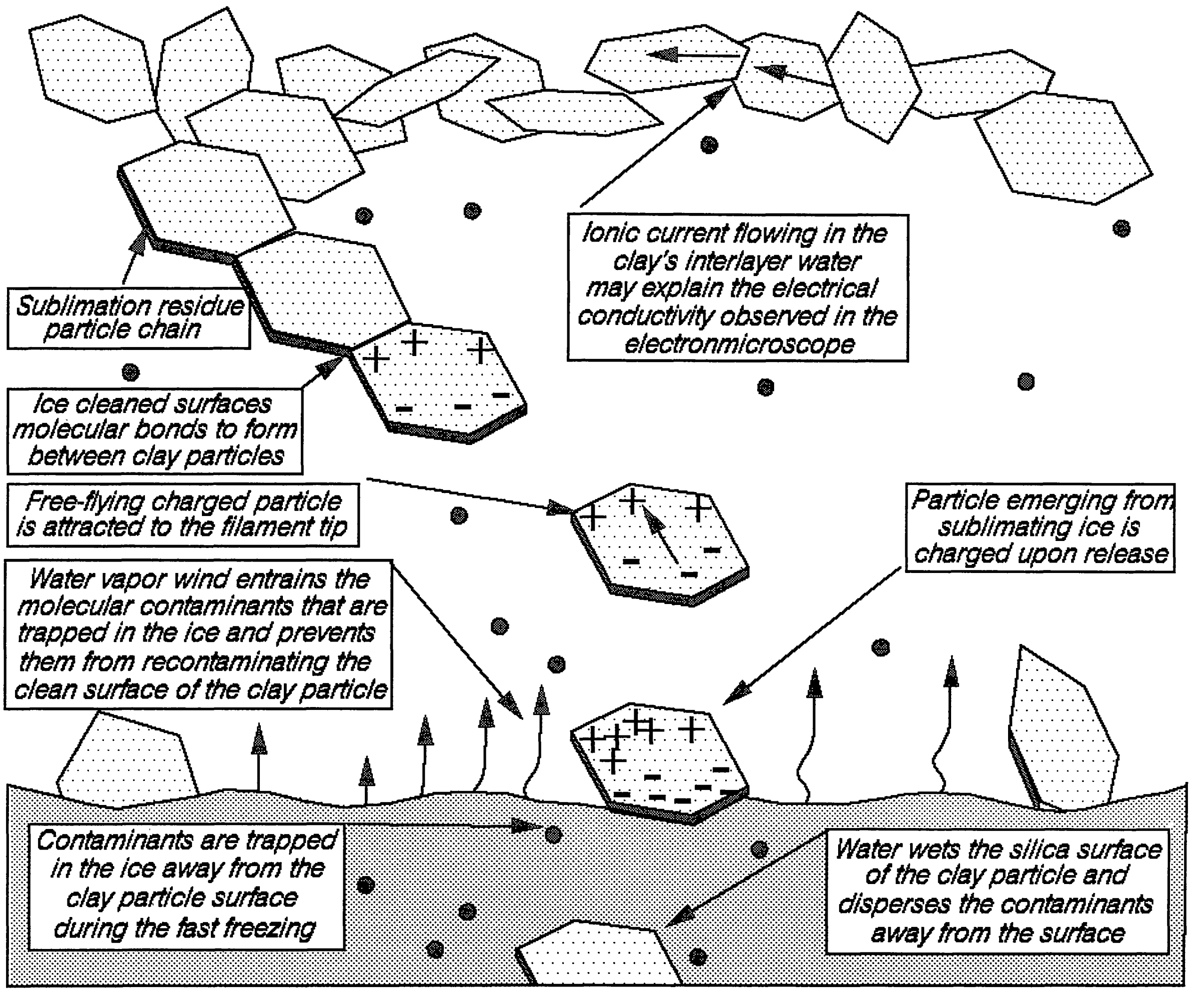

FIG. 29. The structure of clay minerals forming the filamentary structures seen in Fig. 27 with explanations for their major properties (Storrs *et al.*, 1988).

concerns the refractory "irradiation-driven" mantle, which could be centimeters to meters thick. The KOSI experiments assume active areas (no significant mantle) exposed to the many alteration processes occurring in the inner solar system and thus simulate the activity that is relevant to a comet and not that of a dead body. Simulating a dead body would be of relatively little interest. Simulation experiments and the data should be viewed with these cautions in mind.

Although uniquely valuable insights into comet evolution have been observed, in many respects these experiments are incomplete. Could the silicate dust mantle even reach meter dimensions, so that certain meteorites, as well as many micrometeorites, might be cometary? To what extent do comets grade into asteroids? These types of question require that comet simulation experiments be performed with higher amounts of silicate dust than the KOSI experiments. The upper limit for silicates in the KOSI samples material by spraying was 20 to 25 wt%, with higher amounts resulting in very inhomogeneous samples. However, real comet nuclei are processed and modified by solar passage and probably have a very inhomogeneous surface, so an inhomogeneous analogue is probably quite appropriate.

Acknowledgements–We are very grateful to M. Hanner, A. Bar-Nun, and an anonymous reviewer for constructive comments on the paper. WFH gratefully acknowledges support from NASA grant NAG5-7165.

Editorial handling: S. A. Sandford and D. Brownlee

REFERENCES

A'HEARN M. F. AND FESTOU M. C. (1990) The neutral coma. In *Physics and Chemistry of Comets* (ed. W. F. Huebner), pp. 69–112. Springer, Berlin, Germany.

ANDERS E. AND EBIHARA M. (1982) Solar system abundances of the elements. *Geochim. Cosmochim. Acta* **46,** 2363–2380.

ATZEI A., CORADINI M. AND SCHWEHM G. (1992) Rosseta comet-nucleus sample return mission. *Ann. Geophysicae* **10,** 121–122.

BAILEY M. E., CLUBE S. V. M. AND NAPIER W. M. (1986) The origin of comets. *Vistas Astron.* **29,** 53–112.

BAR-NUN A. (1991) Comet simulation experiments as a prelude to the CRAF and Rossetta missions. *Geophys. Res. Lett.* **18,** 289–291.

BAR-NUN A., HERMAN G., LAUFER D. AND RAPPAPORT M. L. (1985) Trapping and release of gases and water ice and implications for icy bodies. *Icarus* **63,** 317–332.

BATTRICK B., ROLFE E. J. AND REINHARD R., EDS. (1986) *20th ESLAB Symposium on the Exploration of Halley's Comet.* European Space Agency, Special Report 250. Noordwijk, The Netherlands.

BENKHOFF J. AND BOICE D. C. (1996) Modeling the thermal properties and the gas flux from a porous, ice–dust body in the orbit of P/Wirtenen. *Planet. Space Sci.* **44,** 665–673.

BENKHOFF J. AND SPOHN T. (1991) Thermal history of the KOSI samples. *Geophys. Res. Lett.* **18,** 261–264.

BENKHOFF J., SEIDENSTICKER K. J., SEIFERLIN K. AND SPOHN T. (1995) Energy analysis of porous water ice under space simulated conditions: Results form the KOSI-8 experiment. *Planet. Space Sci.* **43,** 353–361.

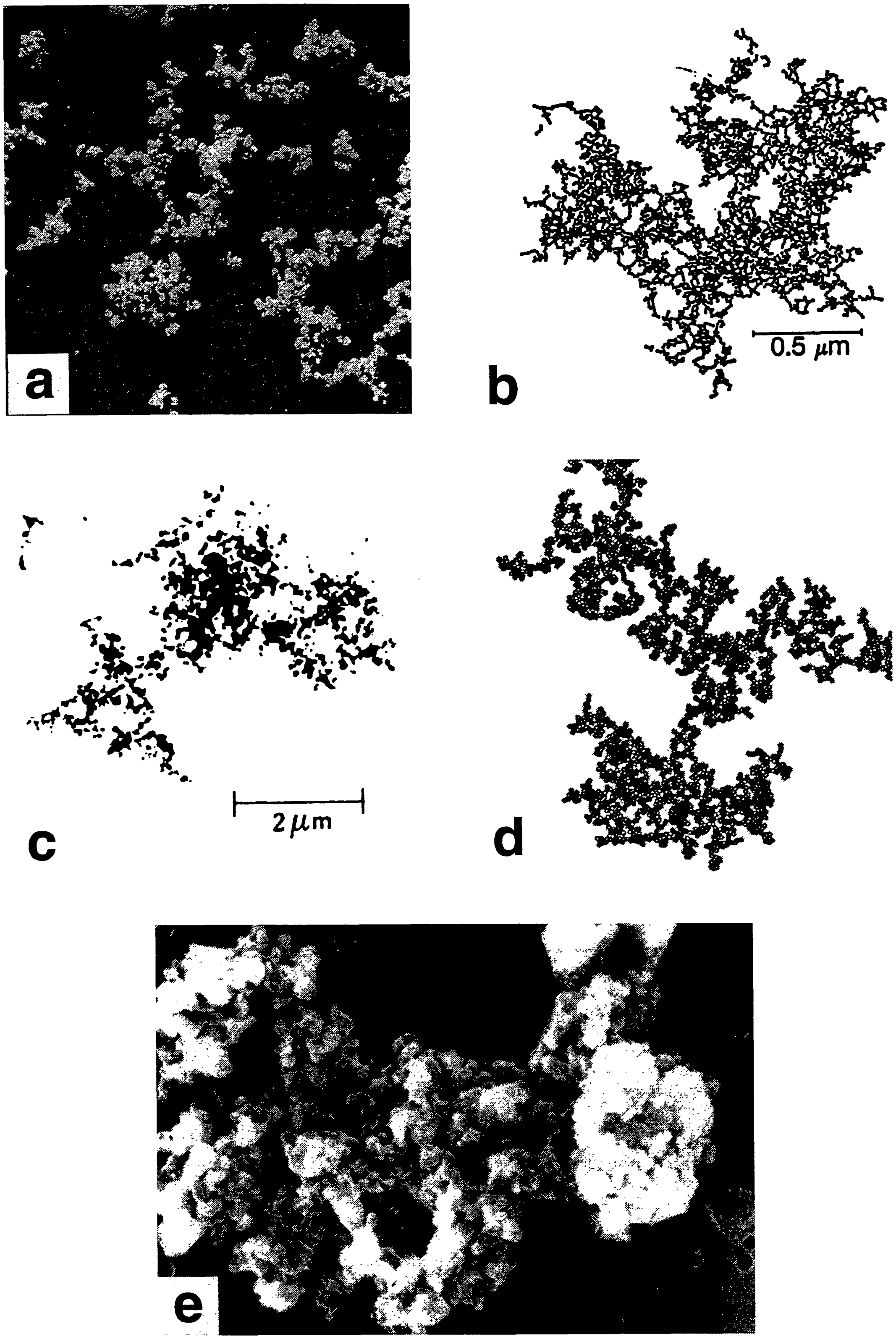

FIG. 30. Possible comet analogue materials according to Donn (1991). (a) Silica clusters formed by the oxidation of silicates in an oxygen–hydrogen flame (horizontal field of view is 1.2 μm). (b) Gold colloidal aggregate. (c) Soot aggregates formed by acetylene combustion (horizontal field of view is 6 μm). (d) Numerical simulation of ballistic cluster–cluster accretion (horizontal field of view is 3 μm). (e) An interplanetary dust particle collected in the stratosphere by a U2 aircraft (horizontal field of view is 10 μm).

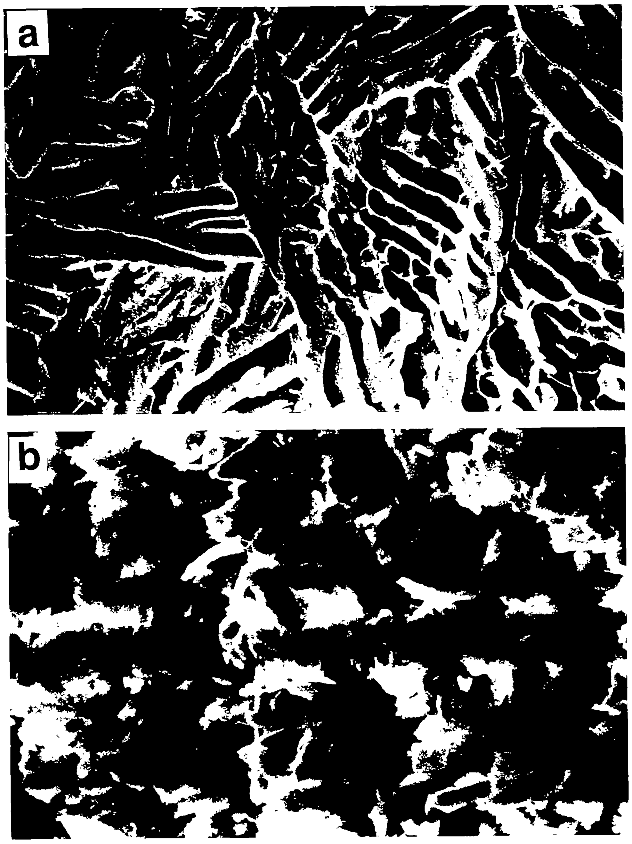

FIG. 31. Scanning electron microscope images of particles emitted from the comet analogue material after collection in the KOSI apparatus. The horizontal field of view is ~400 μm. (a) 100% montmorillonite. (b) 100% olivine. (Courtesy K. Thiel).

BRADLEY J. P. (1988) Analysis of chondritic interplanetary dust thin sections. *Geochim. Cosmochim. Acta* **52,** 889–900.

BRANDT J. C., FARQUHAR R. W., MARAN S. P., NIEDNER M. B., VON ROSENVINGE T. T. (1988). *The International Comet Explorer.* In *Exploration of Halley's Comet* (eds. M. Grewing, F. Praderie and R. Reinhard), pp. 969–980. Springer, Heidelberg, Germany.

BRIN G. D. AND MENDIS D. A. (1979) Dust release and mantle development in comets. *Astrophys. J.* **229,** 402–408.

BROWNLEE D. E. (1985) Cosmic dust: Collection and research. *Ann. Rev. Earth Planet. Sci.* **13,** 147–173.

BROWNLEE D. E., BURNETT D., CLARK B., HANNER M., HÖRZ F., KISSEL J., NEWBURN R., SANDFORD S., SEKANIA Z., TSOU P. AND ZOLENSKY M. (1996) Stardust: Comet and interstellar dust sample return mission. In *Physics and Chemistry of Interplanetary Dust, Astron. Soc. Pacific Conf. Ser. 104* (eds. B. Gustafson and M. Hanners), pp. 223–227. Astronomical Society of the Pacific, San Francisco, California, USA.

CAMPINS H. AND RYAN E. V. (1989) The identification of crystalline olivine in comet silicates. *Astrophys. J.* **341,** 1059–1066.

CAMPINS H. AND SWINDLE T. D. (1998) Expected characteristics of comet meteorites. *Meteoritic. Planet. Sci.* **33,** 1201–1211.

COLANGELI L., BUSSOLETTI E. AND SCHWEHM G. (1989) Physical models of comet nuclei: A review. In *Physics and Mechanics of Comet Materials* (eds. J. Hunt and T. D. Guyenne), pp. 17–22. European Space Agency, Spec. Pub. 302, Paris, France.

COLANGELI L., BUSSOLETTI E. AND MENNELLA V. (1992a) Models of comet nuclei and future space missions. *Ann. Geophysicae* **10,** 178–183.

COLANGELI L., BARATTA G. A., BIANCO A., BUSSOLETTI E., FONTI S., MENNELLA V., OROFINO V. AND STRAZZULLA G. (1992b) The composition of comet materials: Laboratory results. *Ann. Geophysicae* **10,** 184–189.

CORODINI A., CAPACCIONI F., CAPRIA M. T., DE SANCTIS M. C., ESPINASSE S., OROSEI R., SALOMONE M. AND FEDERICO C. (1997a) Transition elements between asteroids and comets I. Thermal evolution models. *Icarus* **129,** 317–336.

CORODINI A., CAPACCIONI F., CAPRIA M. T., DE SANCTIS M. C., ESPINASSE S., OROSEI R., SALOMONE M. AND FEDERICO C. (1997b) Transition elements between asteroids and comets II. From the Kuiper Belt to NEO orbits. *Icarus* **129,** 337–347.

DEGEWI J. AND TEDESCO E. F. (1979) Do comets evolve into asteroids? Evidence from physical studies. In *Comets* (ed. L. L. Wilkening), pp. 665–695. Univ. Arizona, Tucson, Arizona, USA.

DELSEMME A. H., ED. (1977) *Comets, Asteroids, Meteorites.* Univ. Toledo, Toledo, Ohio, USA. 587 pp.

DIVINE N., FECHTIG H., GOMBOSI T. I., HANNER M. S., KELLER H. U., LARSON S. M., MEDIS D. A., NEWBURN R. L., REINHARD R., SEKANINA Z. AND YEOMANS D. K. (1986) The Comet Halley dust and gas environment. *Space Sci. Rev.* **43,** 1–104.

DOBROVOLSKY O. V. AND KAJMAKOW E. (1977) Surface phenomena in simulated comet nuclei. In *Comets, Asteroids, Meteorites* (ed. A. H. Delsemme), pp. 37–46. Univ. Toledo, Toledo, Ohio, USA.

DOBROVOLSKY O. V., IBADINOV K. I., ALIEV S. AND GERASIMENKO S. I. (1986) Thermal regime and surface structure of periodic comet nuclei. In *20th ESLAB Symposium on the Exploration of Halley's Comet, Vol. 2* (eds. B. Battrik, E. J. Rolfe and R. Reinhard), pp. 389–394. European Space Agency, Spec. Pub. 250, Noordwijk, The Netherlands.

DONN B. (1991) The accumulation and structure of comets. In *Comets in the Post-Halley Era* (eds. R. L. Newburn, M. Neugebauer and J. Rahe), pp. 335–359. Kluwer, Dordrecht, The Netherlands.

DONN B. AND HUGHES D. W. (1986) A fractal model of a comet nucleus formed by random accretion. In *20th ESLAB Symposium on the exploration of Halley's Comet, Vol. III* (eds. B. Battrik, E. J. Rolfe and R. Reinhard), pp. 523–524. European Space Agency, Spec. Pub. 250, Noordwijk, The Netherlands.

ESA SP-249 (1986) *The Comet Nucleus Sample Return Mission.* European Space Agency, Spec. Pub. 249.

EIDEN M. J. AND COSTE P. A. (1992) The challenge of sample acquisition in comet environment. *Ann. Geophysicae* **10,** 131–140.

ESPINASSE S., KLINGER J., RITZ C. AND SCHMITT B. (1991) Modeling of the thermal behavior and of the chemical differentiation of comet nuclei. *Icarus* **92,** 350–365.

FANALE F. P. AND SALVAIL J. R. (1984) An idealized short-period comet model: Surface insolation, H_2O flux, and mantle evolution. *Icarus* **60,** 476–511.

FANALE F. P. AND SALVAIL J. R. (1986) A model of comet and gas dust production and non-gravitational force with application to P/Halley. *Icarus* **66,** 154–164.

FARQUHAR R. W., DUNHAM D. W. AND SHAO-CHIAN JEN (1997) Contour mission overview and trajectory design. *Adv. Astron. Sci.* **95,** 921–934.

GOMBOSI T. I. AND HOUPIS H. L. F. (1986) An icy-glue model of comet nuclei. *Nature* **324,** 43–44.

GREENBERG J. M. (1977) From interstellar dust to comets to dust. In *Comets, Asteroids, Meteorites* (ed. A. H. Delsemme), pp. 491–497. Univ. Toledo, Toledo, Ohio, USA.

GREENBERG J. M. (1982) What are comets made of? A model based on interstellar dust. In *Comets* (ed. L. L. Wilkening), pp. 131–163. Univ. Arizona, Tucson, Arizona, USA.

GREENBERG J. M. (1986) Fluffy comets. In *Asteroids, Comets, Meteoroids II* (eds. C-I. Lagerkvist, B. A. Lindblad, H. Lundstedt and H. Rickman), pp. 221–223. Uppsala University, Astronomiska Observatoriet, Sweden.

GREENBERG J. M. AND HAGE J. I. (1990) From interstellar dust to comets: A unification of observational constraints. *Astrophys. J.* **361,** 260–274.

GREWING M., PRADERIE F. AND REINHARD R. (1988) *Exploration of Halley's Comet.* Springer, Heidelberg, Germany. 984 pp.

GRÜN E. AND JESSBERGER E. K. (1990) Dust. In *Physics and Chemistry of Comets* (ed. W. F. Huebner), pp. 113–176. Springer, Berlin, Germany.

GRÜN E., KOCHAN H., RÖSSLER K. AND STÖFFLER D. (1987) Simulation of comet nuclei. In *Diversity and Similarity of Comets,* pp. 501–508. European Space Agency, Spec. Pub. 278, ESA Publ. Div., ESTEC, Noordwijk, The Netherlands.

GRÜN E., KOCHAN H. AND SEIDENSTICKER K. J. (1991a) Laboratory simulation: A tool for comet research. *Geophys. Res. Lett.* **18,** 245–248.

GRÜN E., BENKHOFF J., HEIDRICH R., HESSELBARTH R., KOHL H. AND KÜHRT E. (1991b) Energy balance of the KOSI 4 experiment. *Geophys. Res. Lett.* **18,** 253–256.

GRÜN E. *et al.* (1991c) Laboratory simulation of comet processes: Results from the first KOSI experiments. In *Comets in the Post-Halley Era* (eds. R. L. Newburn, M. Neugebauer and J. Rahe), pp. 277–297. Kluwer, Dordrecht, The Netherlands.

GRÜN E., BENKHOFF J. AND GEBHARD J. (1992) Past, present and future KOSI comet simulation experiments. *Ann. Geophysicae* **10,** 190–197.

GRÜN E. *et al.* (1993) Development of a dust mantle on the surface of an insolated ice-dust mixture: Results from the KOSI -9 experiment. *J. Geophys. Res.* **98,** 15 091–15 104.

HANNER M. S., LYNCH D. K. AND RUSSELL R. W. (1994) The 8–13 micron spectra of comets and the composition of the silicate grains. *Ap. J.* **425,** 274–285.

HESSELBARTH P., KRANKOWSKY D., LÄMMERZAHL P., MAUERSBERGER K., WINKLER A., HSIUNG P. AND RÖSSLER K. (1991) Gas release from ice/dust mixtures. *Geophys. Res. Lett.* **18,** 269–272.

HIRAO K. AND ITOH T. (1986) The planet-A encounters. *Nature* **321,** 294–297.

HOSKINS M., ED. (1997) *The Cambridge Illustrated History of Astronomy.* Cambridge University Press, Cambridge, U.K. 400 pp.

HORANYI M., GOMBOSI T. I., CRAVENS T. E., KÖRÖSMEZEY A., KECSKEMETY, NAGY K. AND SZEGÖ K. (1984) The friable sponge model of comet nuclei. *Astrophys. J.* **278,** 449–455.

HSIUNG P. AND RÖSSLER K. (1989) CO_2 depth profiles in comet model substances of KOSI. In *Proceedings of an International Workshop of Physics and Mechanics of Comet Materials*, (eds. J. Hunt and T. D. Guyenne), pp. 191–196. European Space Agency, Spec. Pub. 302, Paris, France.

HUEBNER W. F. (1965) Uber die Gasproduktion der Kometen. *Z. Astrophys.* **63,** 22–34.

HUEBNER W. F. (1987) First polymer in space identified in Comet Halley. *Science* **237,** 628–630.

HUEBNER W. F., ED. (1990) *Physics and Chemistry of Comets.* Springer, Berlin, Germany. 376 pp.

HUEBNER W. F. AND BOICE D. C. (1992) On the 3D time-dependent modeling of comet nucleus surface layers. *Ann. Geophysicae* **10,** 169–177.

HUEBNER W. F., BOICE D. C., SCHMIDT H. U. AND WEGMANN R. (1991) Structure of the coma: Chemistry and solar wind interaction. In *Comets in the Post-Halley Era, Vol. 2* (eds. R. L. Newburn, M. Neugebauer and J. Rahe), pp. 907–936. Kluwer, Dordrecht, The Netherlands.

HUEBNER W. F., BENKHOFF J., CAPRIA M., CORADINI A., DE SANCTIS C., ENZIAN A., OROSEI R. AND PRIALNIK D. (1998) Results form the comet nucleus model team at the International Space Science Institute, Bern. *COSPAR Proc.* (in press).

HUGHES D. W. (1981) The size, mass, mass loss, and age of Halley's comet. *Mon. Not. Roy. Astron. Soc.* **213,** 103–109.

HUNT J. AND GUYENNE T. D., EDS. (1989) *Proceedings of an International Workshop of Physics and Mechanics of Comet Materials.* European Space Agency, Spec. Pub. 302, Paris France.

IBADINOV K. I. AND ALIEV S. (1987) Sublimation characteristics of H_2O comet nucleus with CO_2 impurities. In *Diversity and Similarity of Comets* (eds. E. J. Rolfe and B. Battrick), pp. 717–719. European Space Agency, Spec. Pub. 278, ESA Publ. Div., ESTEC, Noordwijk, The Netherlands.

IBADINOV KH. I. AND KAJMAKOV E. A. (1970) Formation and destruction of dust matrices during sublimation of dusty ice. *Komety i Meteory* **19,** 20.

IBADINOV KH. I., RAHMONON A. A. AND BJASSO A. SH. (1991) Laboratory simulation of comet structures. In *Comets in the Post-Halley Era* (eds. R. L. Newburn, M. Neugebauer and J. Rahe), pp. 299–311. Kluwer, Dordrecht, The Netherlands.

JACKSON W. M. (1991) Recent laboratory photochemical studies and their relationship to the photochemical formation of comet radicales. In *Comets in the Post-Halley Era* (eds. R. L. Newburn, M. Neugebauer and J. Rahe), pp. 313–332. Kluwer, Dordrecht, The Netherlands.

JESSBERGER H. L. AND KOTTHAUS M. (1989) Compressive strength of synthetic comet nucleus samples. In *Physics and Mechanics of Comet Materials* (eds. J. Hunt and T. D. Guyenne), pp. 141–146. European Space Agency, Spec. Pub. 302, Paris, France.

JESSBERGER E. K., CHRISTORIDIS A. AND KISSEL J. (1988) Aspects of the major element composition of Halley's dust. *Nature* **332,** 691–695.

JEWITT D. C. AND LUU J. (1993) Discovery of candidate Kuiper Belt object 1992 QB_1. *Nature* **362,** 730–732.

JEWITT D. C. AND LUU J. X. (1995) The solar system beyond Neptune. *Astron. J.* **109,** 1867–1873.

JOHNSON R. E. (1990) *Energetic Charged-Particle Interactions with Atmospheres and Surfaces.* Springer-Verlag, Berlin, Germany. 232 pp.

JOHNSON R. E., COOPER J. F., LANZEROTTI L. J. AND STRAZZULA G. (1987) Radiation formation of a non-volatile crust. *Astron. Astrophys.* **187,** 889–892.

KAJMAKOV E. A. AND SHARKOV V. I. (1967) Behavior of water ice containing dust particles. *Komety i Meteory* **15,** 16.

KELLER H. U. (1989), Comets–Dirty snowballs or icy dirtballs? In *Physics and Mechanics of Comet Materials* (eds. J. Hunt and T. D. Guyenne), pp. 39–45. European Space Agency, Spec. Pub. 302, Paris, France.

KELLER H. U. (1990) The Nucleus. In *Physics and Chemistry of Comets* (ed. W. F. Huebner), pp. 13–68. Springer, Berlin, Germany.

KELLER H. U. AND MARKIEWICZ W. J. (1991) KOSI? *Geophys. Res. Lett.* **18,** 249–252.

KELLER H. U., KRAMM R. AND THOMAS N. (1988) Surface features on the nucleus of Comet Halley. *Nature* **331,** 227–231.

KERRIDGE J. F. AND MATTHEWS M. S. S. (1988) *Meteorites and the Early Solar System.* Univ. Arizona Press, Tucson, Arizona, USA. 1269 pp.

KLINGER J. (1980) Influence of a phase transition of ice on the heat and mass balance of comets. *Science* **209,** 271–272.

KLINGER J. (1991) Physical properties of frozen volatiles—Their relevance to the study of comet nuclei. In *Comets in the Post-Halley Era* (eds. R. L. Newburn, M. Neugebauer and J. Rahe), pp. 227–241. Kluwer, Dordrecht, The Netherlands.

KLINGER J., BENEST D., DOLLFUS A. AND SMOLUCHOWSKI R., EDS. (1985) *Ices in the Solar System.* Reidel, Dordrecht, The Netherlands. 954 pp.

KLINGER J., BENKHOFF J., ESPINASSE S., GRÜN E., IP W., JOO F., KELLER H. U., KOCHAN H., KOHL H., RÖSSLER K., SEBOLDT W., SPOHN T. AND THIEL K. (1989) How far do results of recent simulation experiments fit current models of comet nuclei? *Proc. Lunar Planet. Sci. Conf.* **19th,** 493–497.

KOCHAN H. AND JUNGLUS CH. (1993) From the space environment to the planetary surface, from hardware tests to physical experiments—a changing utilization of space simulators. In *Proceedings of the 2nd International Symposium on Environmental Testing for Space Programmes*, pp. 483–489. European Space Agency, WPP-066, Paris, France.

KOCHAN H. AND KOERVER W. (1991) Dust emission phenomena of comet analogues. *Adv. Space Res.* **11,** (12)161–(12)174.

KOCHAN H. *et al.* (1989a) Comet simulation experiments in the DFVLR space simulators. *Adv. Space Res.* **9,** (3)113–(3)122.

KOCHAN H. *et al.* (1989b) Laboratory simulation of a comet nucleus: Experimental setup and first results. *Proc. Lunar Planet. Sci. Conf.* **19th,** 487–492.

KOCHAN H., RÖESSLER K., RATCKE L., HEYLE M., HELIMANN H. AND SCHWEHM G. (1989c) Crustal strength of different model comet materials. In *Physics and Mechanics of Comet Materials* (eds. J. Hunt and T. D. Guyenne), pp. 115–119. European Space Agency, Spec. Pub. 302, Paris, France.

KOCHAN H., MARKIEWICZ W. J. AND KELLER H. U. (1991) KOSI: Gas drag derived from ice/dust-particle trajectories. *Geophys. Res. Lett.* **18,** 273–276.

KOLOKOVA L. AND JOCKERS K. (1997) Composition of comet dust from polarization spectra. *Planet. Space Sci.* **45,** 1543–1550.

KÖLZER G., GRÜN E., KOCHAN H., LÄMMERZAHL P. AND THIEL K. (1995) Dust particle dynamics from insolated ice/dust mixtures: Results from the KOSI 5 experiment. *Planet. Space. Sci.* **43,** 391–407.

KÖMLE N. I., STEINER G., BAGUHL M., KOHLE H., KOCHAN H. AND THIEL K. (1991) The effect of non-volatile porous layers on temperature and vapor pressure of underlying ice. *Geophys. Res. Lett.* **18,** 265–268.

KÖMLE N. I., KARGL G., THIEL K. AND SEIFERLIN K. (1996) Thermal properties of comet ices and sublimation residua including organics. *Planet. Space Sci.* **44,** 675–689.

KÖMLE N. I., BALL A. J., KARGL G., STÖCKER J., THIEL M., JOLLY H. S., DZIRUNI M. AND ZARNECKI J. C. (1997) Using the anchoring device of a comet lander to determine surface mechanical properties. *Planet. Space Sci.* **45,** 1515–1538.

KOSSACKI K. J., KÖMLE N. I., KARGL G. AND STEINER G. (1994) The influence of grain sintering on the thermoconductivity of porous ice. *Planet. Space Sci.* **42,** 383–389.

KOUCHI A., YAMAMOTO T., KOZASA T., KURODA T. AND GREENBERG J. M. (1994) Conditions for condensation and preservation of amorphous ice and crystallinity of astrophysical ices. *Astron. Astrophys.* **290,** 1009–1018.

KRUEGER F. R., KORTH A. AND KISSEL J. (1991) The organic matter of comet Halley as inferred by joint gas phase and solid phase analyses. *Space Sci. Rev.* **56,** 167–175.

KÜHRT E. AND KELLER H. U. (1994) The formation of comet surface crusts. *Icarus* **109,** 121–132.

LAFONTAINE J. DE, CHAMPETIER C., RÉGNIER P. AND SERRANO J. (1992) The importance of comet models in the design of the Rosseta mission. *Ann. Geophysicae* **10,** 123–130.

LAGERKVIST C-I., LINDBLAD A., LUNDSTEDT H. AND RICKMAN H. (1986) *Asteroids, Comets, Meteroids II.* Uppsala University, Astronomiska Observatoriet, Sweden. 619 pp.

LEWIS J. S. AND PRINN R. G. (1980) Kinetic inhibition of CO and N_2 reduction in the solar nebula. *Astrophys. J.* **238,** 357–364.

LORENZ E., KNOLLENBERG J., KROKER H. AND KÜHRT E. (1995) IR observations of KOSI samples. *Planet. Space Sci.* **43,** 341–351.

MARKIEWICZ W. J., SKOROV YU. V., KELLER H. U. AND KÖMLE N. I. (1998) Evolution of ice surfaces within porous near-surface layers on comet nuclei. *Planet. Space Sci.* **46,** 357–366.

MAUERSBERGER K., MICHEL H-J., KRANKOWSKY D., LÄMMERZAHL P. AND HESSELBARTH P. (1991) Measurement of the volatile component in particles emitted from an ice/dust mixture. *Geophys. Res. Lett.* **18,** 277–280.

MAAS D., KRUEGER F. R. AND KISSEL J. (1990) Mass and sensity of silicate- and CHON-type particles released by comet P/Halley. In *Asteroids, Comets, Meteoroids III* (eds. C. I. Langerkvist, H. Rickman, B. A. Lindblad and M. Lindgren), pp. 389–392. Uppsala Univ., Astronomiska Observatoriet, Sweden.

MCDONNELL J. A. M. *et al.* (1987) The dust distribution within the inner coma of Comet P/Halley 1982i: Encounter by *Giotto*'s impact detectors. *Astron. Astrophys.* **187,** 719–741.

MCKINNON I. D. R. AND RIETMEIJER F. J. M. (1987) Mineralogy of chondritic interplanetary dust particles. *Rev. Geophys.* **25,** 1527–1553.

MEKLER YU., PRIALNIK D. AND PODOLAK D. K. (1990) Evaporation from a porous comet nucleus. *Astrophys. J.* **356,** 682–686.

MÖHLMANN D. (1995) Comet activity and nucleus models. *Planet. Space Sci.* **43,** 327–332.

MÖHLMANN D. (1996) Comet activity and nucleus modelling: A new approach. *Planet. Space Sci.* **44,** 541–546.

MUIRHEAD B. K., KERIDGE S. J., WEISMANN P. R., GREEN J. R., SABAHI D., TAN-WANG G. H. AND GRIMES J. H. (1997) Champollion/Deep Space 4: A comet lander and sample return technology demonstration mission (abstract). *Bull. Amer. Astron. Soc.* **29,** 1032.

NEWBURN R. L., NEUGEBAUER M. AND RAHE J. (1991) *Comets in the Post-Halley Era.* Kluwer Academic Publishers, Dordrecht, The Netherlands. 1360 pp.

OEHLER A. AND NEUKUM G. (1991) Visible and near IR albedo measurements of ice/dust mixtures. *Geophys. Res. Lett.* **18,** 253–256.

OEHLER A., LINDERMEIR E., HASCHBERGER P. AND TANK V. (1992) Laboratory experiments for absolute temperature sounding of cold comet surfaces using an IR Fourier transform spectrometer. *Ann. Geophysicae* **10,** 235–240.

OORT J. H. (1950) The structure of the cloud of comets surrounding the solar system, and an hypothesis concerning its origin. *Bull. Astron. Inst. Neth.* **11,** 91–110.

ÖPIK E. J. (1971) Comet families and transneptunian planets. *Irish Astron. J.* **10,** 35–92.

ORÓ J. (1961) Comets and the formation of biochemical compounds on the primitive Earth. *Nature* **190,** 389–390.

PONNAMPERUMA C., ED. (1981) *Comets and the Origin of Life, Proceedings of the Fifth College Park Colloquium on Chemical Evolution.* D. Reidel, Dordrecht, The Netherlands. 277 pp.

PRIALNIK D. (1992) Crystallization, sublimation, and gas release in the interior of a porous comet nucleus. *Astrophys. J.* **388,** 196–202.

PRIALNIK D. AND BAR-NUN A. (1988). The formation of a permanent dust mantle and its effect on comet activity. *Icarus* **74,** 272–283.

PRINN R. G. AND FEGLEY B. (1989) Solar nebular chemistry: Origin of planetary, satellite and comet volatiles. In *Origin and Evolution of Planetary and Satellite Atmospheres* (eds. S. K. Atreya, J. B. Pollack and M. S. Matthews), pp. 78–136. Univ. Arizona Press, Tucson, Arizona, USA.

RATKE L. AND KOCHAN H. (1989) Fracture mechanical apsects of dust emission processes from a model comet surface. In *Physics and Mechanics of Comet Materials* (eds. J. Hunt and T. D. Guyenne), pp. 121–128. European Space Agency, Spec. Pub. 302, Paris, France.

RAYMAN M. D., CHADBOURNE P. A., CULWELL J. S. AND WILLIAMS S. N. (1998) Mission design for Deep Space 1: A low-thrust technology validation mission. *IAA Inter. Conf. Low-Cost Planetary Missions, Pasadena, California, April 27–May 1, IAA-L98-0502* **3rd,** pp. 1–10.

REINHARD R. (1988) The *Giotto* mission to Halley's comet. In *Exploration of Halley's Comet* (eds. M. Grewing, F. Praderie and R. Reinhard), pp. 949–958. Springer, Heidelberg, Germany.

RICKMAN H. (1986) Masses and densities of comets Halley and Kopff. In *The Comet Nucleus Sample Return Mission.* European Space Agency, Spec. Pub. 249, Paris, France.

RICKMAN H. (1989) The nucleus of comet Halley: Surface structure, mean density, gas and dust production. *Adv. Space Res.* **9,** 59–71.

RICKMAN H. (1991) The thermal history and structure of comet nuclei. In *Comets in the Post-Halley Era, Vol. 2* (eds. R. L. Newburn, M. Neugerbauer and J. Rahe), pp. 733–760. Kluwer Academic Publishers, Dordrecht, The Netherlands.

RICKMAN H. (1992) Comet nuclei—recent gas flux modeling and applications. *Ann. Geophysicae* **10,** 157–168.

RICKMAN H. AND HUEBNER W. F. (1990) Comet formation and evolution. In *Physics and Chemistry of Comets* (ed. W. F. Huebner), pp. 245–303. Springer, Berlin, Germany.

ROLFE E. J. AND BATTRICK B., EDS. (1987) *Symposium on the Diversity and Similarity of Comets.* European Space Agency, Spec. Pub. 278, ESA Publ. Div., ESTEC, Noordwijk, The Netherlands.

ROSS J. E. AND ALLER L. H. (1976) The chemical composition of the Sun. *Science* **191,** 1223–1229.

RÖSSLER K., HSIUNG P., KOCHAN H., HELLMANN H., DÜREN H., THIEL K. AND KÖLZER G. (1990) A model comet made from mineral dust and H_2O–CO_2 ice: Sample preparation development. *Proc. Lunar Planet. Sci. Conf.* **20th,** 379–388.

RÖSSLER K., SAUER M. AND SCHULTZ R. (1992a) Gaseous products from VUV photolysis of comet solids. *Ann. Geophysicae* **10,** 226–231.

RÖSSLER K., EICH G., KLINGER E. AND TRIMBORN P. (1992b) Changes of natural isotopic abundances in the KOSI comet simulation experiments. *Ann. Geophysicae* **10,** 232–234.

RÖSSLER K., BENIT J. AND HEYL M. (1992c) Crust formation in comet analogues. *Ann. Geophysicae* **10,** 217–221.

SAGDEEV R. Z. (1988) The Vega mission to Halley's comet. In *Exploration of Halley's Comet* (eds. M. Grewing, F. Praderie and R. Reinhard), pp. 959–964. Springer, Heidelberg, Germany.

SAGDEEV R. Z., AVANESOV G., ZIMAN Y. L., MOROZ V. I., TARNOPOLSKY V. A., ZHUKOV B. S., SHAMIS V. A., SMITH B. A. AND TOTH I. (1986) TV experiment of the *Vega* mission: Photometry of the nucleus and the inner coma. In *20th ESLAB Symposium on the Exploration of Halley's Comet* (eds. B. Battrick, E. J. Rolfe and R. Reinhard), pp. 317–326. European Space Agency, Special Report 250. Noordwijk, The Netherlands.

SANDFORD S. A. AND WALKER R. M. (1985) Laboratory infrared transmission spectra of individual interplanetary dust particles from 2.5 to 25 microns. *Astrophys. J.* **291,** 838–851.

SAUNDERS R. S., FANALE F., PARKER T. J., STEPHENS I. B. AND SUTTON S. (1986) Properties of filamentary sublimation residues from dispersion of clay in ice. *Icarus* **66,** 94–104.

SCHMITT B., DE BERGH C. AND FESTOU M., EDS. (1998) *Solar System Ices.* Kluwer Academic Publishers, Dordrecht, The Netherlands. 826 pp.

SEIDENSTICKER K. J. AND KOCHAN H. (1992) Experiments with comet analogues at the DLR. *Ann. Geophysicae* **10,** 198–205.

SEKININA Z. (1997) The problem of split comets revistited. Astron. Astrophys. **318,** L5–L8.

SHULMAN E. M. (1972) The evolution of comet nuclei. In *The Motion, Evolution of Orbits, and Origin of Comets* (eds. G. A. Chebotarev, E. I. Kazimirchak–Polanskaya and B. G. Marsden), pp 271–276. Reidel, Dordrecht, The Netherlands.

SKOROV YU. V. AND RICKMAN H. (1995) A kinetic model of gas flow in a porous comet mantle. *Planet. Space Sci.* **43,** 1587–1594.

SMOLUCHOWSKI R. (1981) Amorphous ice and the behavior of comet nuclei. *Astrophys. J.* **244,** L31–L43.

SPOHN T. AND BENKHOFF J. (1990) Thermal history models for KOSI sublimation experiments. *Icarus* **87,** 358–371.

SPOHN T., SEIFERLIN K. AND BENKHOFF J. (1989a) Thermal conductivities and diffusivities of porous ice samples at low pressure and temperatures and possible modes of heat transfer near surface layers of comets. In *Physics and Mechanics of Comet Materials* (eds. J. Hunt and T. D. Guyenne), pp. 77–82. European Space Agency, Spec. Pub. 302, Paris, France.

SPOHN T., BENKHOFF J., KLINGER J., GRÜN E. AND KOCHAN H. (1989b) Thermal modelling of two KOSI comet nucleus simulation experiments. *Adv. Space Res.* **9,** 127–131.

STERN S. A. (1988) Collision in the Oort cloud. *Icarus* **73,** 499–507.

STERN S. A. AND CAMPINS H. (1996) Chiron and the Centaurs: Escapees from the Kuiper belt. *Nature* **382,** 507–510.

STEPHEN J. R. AND RUSSELL R. W. (1979) Emission and extinction of ground and vapor-condensed silicates from 4 to 14 microns and the 10 micron silicate feature. *Ap. J.* **228,** 780–786.

STÖFFLER D. (1991) Concepts for the curation, primary examination, and allocation of comet nucleus samples by a comet sample receiving laboratory. *Space Sci. Rev.* **56,** 203–211.

STÖFFLER D. AND DÜREN H. (1992) Comet analogue material: Types, tests, and results. *Ann. Geophysicae* **10,** 206–216.

STÖFFLER D., DÜREN H., KNÖKER J., HISCHE R. AND BISCHOFF A. (1991) Comet analogue material: Preparation, composition, and thin section petrography. *Geophys. Res. Lett.* **18,** 285–288.

STORRS A. D., FANALE F., SAUNDERS R. S. AND STEPHENS J. B. (1988) The formation of filamentary sublimate residues (FSR) from mineral grains. *Icarus* **76,** 493–512.

STRAZZULA G. AND JOHNSON R. E. (1991) Irradiation effects on comets and comet debris. In *Comets in the Post-Halley Era, Vol. 1* (eds. R. L. Newburn, M. Neugerbauer and J. Rahe), pp. 243–275. Kluwer Academic Publishers, Dordrecht, The Netherlands.

STRAZZULA G., BARRATTA G. A., JOHNSON R. E. AND DONN B. (1991) The primordial comet mantle: Irradiation production of a stable, organic crust. *Icarus* **91,** 101–104.

THIEL K., KÖLZER G. AND KOHL H. (1991) Dust emission of mineral/ice mixtures: Residue structure and dynamical parameters. *Geophys. Res. Lett.* **18,** 281–284.

THIEL K., SCHWEHM G. AND WEISHAUPT U. (1989) Comet simulation experiments in the DFVLR space simulators. *Adv. Space Res.* **9,** 375–390.

THIEL K., KÖLZER G., KOCHAN H., LÄMMERZAHL P. AND LORENZ E. (1995) Phenomenology and dynamic behavior of the dust component in the KOSI experiments. *Planet. Space Sci.* **43,** 375–390.

TOKUNAGA A. T., GOLISH W. F., GRIEP D. M., KAMINSKI C. AND HANNER M. S. (1986) The NASA infrared telescope facility Comet Halley monitoring program. I: Preperihelion results. *Astron. J.* **92,** 1183–1190.

VANYSEK V. (1991) Isotopic ratios in comets. In *Comets in the Post-Halley Era, Vol. 1* (eds. R. L. Newburn, M. Neugerbauer and J. Rahe), pp. 879–895. Kluwer Academic Publishers, Dordrecht, The Netherlands.

WALLIS M. K. AND MACPHERSON A. K. (1981) On the outgassing and jet thrust of snowball comets. *Astron. Astrophys.* **98,** 45–49.

WEISSMAN P. R. (1986) Are comet nuclei primordial rubble piles? *Nature* **320,** 242–244.

WEISSMAN P. R. AND KIEFFER H. H. (1981) Thermal modelling of comet nuclei. *Icarus* **47,** 302–311.

WEISSMAN P. R., A'HEARN M. F., MCFADDEN L. A. AND RICKMAN H. (1989) Evolution of comets into asteroids. In *Asteroids II* (eds. R. P. Binzel, T. Gehrels and M. S. Matthews), pp. 880–920. Univ. Arizona Press, Tucson, Arizona, USA.

WETHERILL G. W. (1991) End products of comet evolution: Comet origin of Earth-crossing bodies of asteroidal appearance. In *Comets in the Post-Halley Era, Vol. 1* (eds. R. L. Newburn, M. Neugerbauer and J. Rahe), pp. 537–556. Kluwer Academic Publishers, Dordrecht, The Netherlands.

WHIPPLE F. L. (1950) The comet model I. The acceleration of Comet Encke. *Astrophys. J.* **111,** 375–394.

WHIPPLE F. L. (1951) The comet model II. Physical relations for comets and meteorites. *Astrophys. J.* **113,** 464–474.

WILKENING L. L. (1982) *Comets.* Univ. Arizona Press, Tucson, Arizona, USA. 766 pp.